INTERNATIONAL JOURNAL FOR NUMERICAL METHODS IN ENGINEERING
Int. J. Numer. Meth. Engng. 2000; **48**:289–313

The mathematical shell model underlying general shell elements

Dominique Chapelle[1,*,†] and Klaus-Jürgen Bathe[2]

[1] *INRIA-Rocquencourt - B.P. 105 - 78153 Le Chesnay Cedex, France*
[2] *Massachusetts Institute of Technology, Cambridge MA 02139, U.S.A.*

SUMMARY

We show that although no actual mathematical shell model is explicitly used in 'general shell element' formulations, we can identify an implicit shell model underlying these finite element procedures. This 'underlying model' compares well with classical shell models since it displays the same asymptotic behaviours—when the thickness of the shell becomes very small—as, for example, the Naghdi model. Moreover, we substantiate the connection between general shell element procedures and this underlying model by mathematically proving a convergence result from the finite element solution to the solution of the model. Copyright © 2000 John Wiley & Sons, Ltd.

KEY WORDS: shell model; finite element discretization; degenerated solid; asymptotic behaviour

1. INTRODUCTION

Since the early development of practical finite element analysis procedures, a primary objective was to analyse complex shell structures [1–4]. In today's practice, of course, shell structures are abundantly solved in many industries, including the automotive, aircraft and civil engineering environments. However, although shell analyses are widely conducted, the quest for improved analysis procedures continues. To formulate shell finite element discretizations, in essence, three different approaches can be followed [1–4].

In the first approach, the shell behaviour is seen as a superposition of membrane and plate bending actions. Finite elements are constructed by simply combining plate bending and plane stress stiffness matrices. The resulting shell elements, however, are of low performance in accuracy because curvature effects are not included and the plate bending and membrane behaviour is only coupled at the nodal points. Much more effective finite element shell analysis procedures are now available.

*Correspondence to: Dominique Chapelle, INRIA-Rocquencourt, B.P.105 - 78153 Le Chesnay Cedex, France
†E-mail: dominique.chapelle@inria.fr

Received 20 December 1998
Revised 24 October 1999

The second approach is based on using a specific shell theory and discretizing the corresponding variational formulation. If the shell theory contains high-order derivatives, the finite element discretization requires corresponding nodal point variables beyond the usual nodal point displacements and rotations. This requirement results in difficulties when more complex shell structures, that for example include beam stiffeners, need be modelled. Another disadvantage of such an approach is that if the shell theory is only applicable to certain shell geometries or analysis conditions, the finite element formulation is, of course, subject to the same restrictions.

In practice, a very general finite element formulation that can be used for the analysis of virtually any thin or moderately thick shell and in linear or non-linear analysis conditions is most attractive. The basis of such a formulation is provided by the approach of degenerating the three-dimensional continuum to shell behaviour. In this approach, the mid-surface of the three-dimensional continuum is identified and the basic assumptions are that fibres straight and normal to the mid-surface prior to the deformation remain straight during the deformation, and that the stress normal to the shell mid-surface is zero throughout the shell motion. With these assumptions, the construction of a displacement-based finite element discretization is straightforward. While this formulation is only directly effective in very restrictive cases [2, 5], the formulation does provide the basis for mixed finite element methods which are effective for general shell analyses [1, 2, 6, 7]. Specifically, the complete range of membrane and bending-dominated shell structures can be solved with these methods.

In order to reach more effective shell finite element discretization procedures, it is paramount to perform thorough mathematical analyses of the discretization schemes. If the finite element method has been derived based upon a specific shell theory, clearly, the mathematical analysis is concerned with the issues of consistency, stability and convergence measured using that theory. However, in the general approach described above, the shell finite element analysis procedure is obtained directly from three-dimensional discretization subject to the kinematic and stress assumptions mentioned, without the use of a specific shell theory. Since the shell theory is not known, a complete mathematical analysis is difficult to perform and a comparison with other shell mathematical models cannot be directly achieved.

The objective of this paper is to identify the two-dimensional mathematical shell model underlying the general three-dimensional shell analysis approach, to analyse this mathematical model, to compare the model with other well-known shell models, and finally give convergence results of the displacement-based finite element discretization scheme to the solution of the model. The main results were already announced by the authors in Reference [8], and are now fully developed and substantiated in the present paper.

The paper is organized in the following way. In Section 2, we give some definitions and notation regarding the shell geometry and deformations. Then in Section 3, we derive ‘the underlying two-dimensional mathematical model’ of the general three-dimensional shell analysis approach. This derivation is followed in Section 4 by mathematical analyses of the model, specifically, with respect to membrane and bending-dominated behaviours, and with respect to the asymptotic behaviour as the thickness of the shell domain becomes very small. In particular, we conclude that the underlying two-dimensional shell model displays the same asymptotic behaviour as the Naghdi shell model. In Section 5, we then show that the general three-dimensional shell element procedure converges to the solution of the underlying two-dimensional model as the mesh is refined. Finally, in Section 6, we present our conclusions regarding this work.

2. GEOMETRY AND NOTATION

In what follows, we assume that the shell mid-surface, $\mathscr{S}$, can be defined by a single chart $\boldsymbol{\phi}$, which is a one-to-one smooth mapping from $\bar{\Omega}$ into $\mathbb{R}^3$, where Ω denotes an open domain of $\mathbb{R}^2$ called 'reference domain' and thus $\mathscr{S} = \boldsymbol{\phi}(\bar{\Omega})$, see Figure 1 ($\bar{\Omega}$ denotes the closure of Ω, i.e. the union of Ω and its boundary $\partial\Omega$). We now briefly recall the classical definitions and notation of differential geometry that we need for our purposes, see References [3, 9] for more details. We use the Einstein convention on the summation of repeated indices, with the values of indices ranging in $\{1,2\}$ for Greek symbols and in $\{1,2,3\}$ for Roman symbols. Let the covariant base vectors of the tangential plane be defined by

$$\mathbf{a}_\alpha \stackrel{\text{def}}{=} \frac{\partial \boldsymbol{\phi}(\xi_1, \xi_2)}{\partial \xi_\alpha}$$

with the contravariant base vectors (of the tangential plane) given by

$$\mathbf{a}_\alpha \cdot \mathbf{a}^\beta = \delta_\alpha^\beta$$

where δ denotes the Kronecker symbol. The unit normal vector is

$$\mathbf{a}_3 = \frac{\mathbf{a}_1 \times \mathbf{a}_2}{\|\mathbf{a}_1 \times \mathbf{a}_2\|}$$

The first fundamental form of the surface is given by

$$a_{\alpha\beta} \stackrel{\text{def}}{=} \mathbf{a}_\alpha \cdot \mathbf{a}_\beta$$

or alternatively in contravariant form by

$$a^{\alpha\beta} \stackrel{\text{def}}{=} \mathbf{a}^\alpha \cdot \mathbf{a}^\beta$$

The second fundamental form is defined by

$$b_{\alpha\beta} \stackrel{\text{def}}{=} \mathbf{a}_3 \cdot \mathbf{a}_{\alpha,\beta}$$

and the third fundamental form by

$$c_{\alpha\beta} \stackrel{\text{def}}{=} b_\alpha^\lambda b_{\lambda\beta}$$

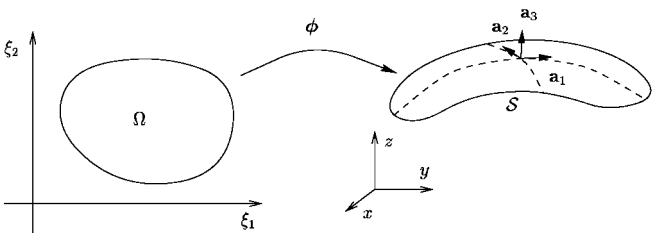

Figure 1. Definition of the mid-surface by a chart.

where we recall that $b_\alpha^\beta \stackrel{\text{def}}{=} a^{\beta\lambda} b_{\lambda\alpha}$. The following symbol appears in surface measures:

$$a \stackrel{\text{def}}{=} \|\mathbf{a}_1 \times \mathbf{a}_2\|^2 = a_{11}a_{22} - (a_{12})^2$$

and indeed we denote

$$\mathrm{d}S \stackrel{\text{def}}{=} \sqrt{a}\,\mathrm{d}\xi_1\,\mathrm{d}\xi_2$$

The covariant differentiation on the mid-surface is denoted by a vertical bar (like in '$v_{\alpha|\beta}$', see Reference [9]).

The geometry of the shell is defined by its mid-surface and a parameter representing the thickness of the three-dimensional medium lying around this surface. For simplicity of discussion we henceforth consider shells of constant thickness, denoted by t. We define the t-dependent domain

$$\Lambda_t \stackrel{\text{def}}{=} \Omega \times]-t/2, t/2[$$

The geometry of the shell can then be described by the chart $\mathbf{\Phi}$, the mapping from $\bar{\Lambda}_t$ into $\mathbb{R}^3$ defined by

$$\mathbf{\Phi}(\xi_1, \xi_2, \xi_3) = \boldsymbol{\phi}(\xi_1, \xi_2) + \xi_3 \mathbf{a}_3(\xi_1, \xi_2)$$

This parametrization defines a system of curvilinear co-ordinates. We can therefore introduce the three-dimensional covariant base vectors

$$\mathbf{g}_i \stackrel{\text{def}}{=} \frac{\partial \mathbf{\Phi}}{\partial \xi_i}$$

which immediately gives

$$\begin{cases} \mathbf{g}_\alpha = (\delta_\alpha^\lambda - \xi_3 b_\alpha^\lambda)\mathbf{a}_\lambda \\ \mathbf{g}_3 = \mathbf{a}_3 \end{cases} \tag{1}$$

From this we can obtain the expression of the components of the three-dimensional metric tensor

$$\begin{cases} g_{\alpha\beta} = \mathbf{g}_\alpha \cdot \mathbf{g}_\beta = a_{\alpha\beta} - 2\xi_3 b_{\alpha\beta} + \xi_3^2 c_{\alpha\beta} \\ g_{\alpha 3} = \mathbf{g}_\alpha \cdot \mathbf{g}_3 = 0 \\ g_{33} = \mathbf{g}_3 \cdot \mathbf{g}_3 = 1 \end{cases} \tag{2}$$

The contravariant three-dimensional base vectors are defined by

$$\mathbf{g}_i \cdot \mathbf{g}^j = \delta_i^j$$

hence

$$\begin{cases} \mathbf{g}_\alpha \cdot \mathbf{g}^\beta = \delta_\alpha^\beta \\ \mathbf{g}^3 = \mathbf{a}_3 \end{cases}$$

The definition of the twice-contravariant components of the metric tensor

$$g^{ij} \stackrel{\text{def}}{=} \mathbf{g}^i \cdot \mathbf{g}^j$$

gives, in particular,

$$\begin{cases} g^{\alpha 3} = 0 \\ g^{33} = 1 \end{cases} \tag{3}$$

Finally, the volume measure is expressed as

$$\mathrm{d}V \overset{\text{def}}{=} \sqrt{g}\,\mathrm{d}\xi_1\,\mathrm{d}\xi_2\,\mathrm{d}\xi_3$$

with

$$g \overset{\text{def}}{=} [(\mathbf{g}_1 \times \mathbf{g}_2)\cdot\mathbf{g}_3]^2 = a(1 - 2H\xi_3 + K\xi_3^2)^2$$

where H and K, respectively, denote the mean and Gaussian curvature of the surface (i.e. the mean and the product, respectively, of the principal curvatures). We note here that the mapping $\mathbf{\Phi}$ is well defined (hence so is the system of curvilinear co-ordinates) provided that the expression $1 - 2H\xi_3 + K\xi_3^2$ is always strictly positive. This is clearly equivalent to requiring that

$$t < 2 \inf_{(\xi_1,\xi_2)\in\bar{\Omega}} |R_{\min}(\xi_1, \xi_2)| \tag{4}$$

where $R_{\min}(\xi_1, \xi_2)$ is the radius of curvature of smallest modulus of the surface at point $\boldsymbol{\phi}(\xi_1, \xi_2)$. We henceforth suppose that condition (4) is satisfied.

3. DERIVATION OF THE 'UNDERLYING 2D-MODEL'

General shell element procedures are inferred from three-dimensional formulations using two basic assumptions [1, 2, 4]:

A-1. The displacements considered are such that, at nodes, the material line normal to the mid-surface in the original configuration remains straight and unstretched during the deformations (kinematical assumption).
A-2. The stresses in the direction normal to the mid-surface are assumed to be zero.

Of course, in practice, using assumption A-1, interpolation is employed between nodal points and, when enforcing assumption A-2, the normal direction used (at the numerical integration points) is given by the interpolation of the nodal normal vectors, see Section 5 for more details on the interpolation.

We henceforth consider an isotropic linear elastic material and we use a constitutive law inferred from assumption A-2. The three-dimensional (3D) variational formulation reads

$$A^{(3D)}(\mathbf{U};\mathbf{V}) = F^{(3D)}(\mathbf{V}), \quad \forall\mathbf{V} \tag{5}$$

The bilinear form $A^{(3D)}$ denotes the virtual work of internal forces. Using the curvilinear coordinate system, it can be written

$$A^{(3D)}(\mathbf{U};\mathbf{V}) \overset{\text{def}}{=} \int_{\Lambda_t} [C^{\alpha\beta\lambda\mu} e_{\alpha\beta}(\mathbf{U}) e_{\lambda\mu}(\mathbf{V}) + D^{\alpha\beta} e_{\alpha 3}(\mathbf{U}) e_{\beta 3}(\mathbf{V})]\,\mathrm{d}V$$

where the e_{ij}'s denote the components of the linearized elastic strains and

$$C^{\alpha\beta\lambda\mu} \stackrel{\text{def}}{=} \frac{E}{2(1+v)}\left(g^{\alpha\lambda}g^{\beta\mu} + g^{\alpha\mu}g^{\beta\lambda} + \frac{2v}{1-v}g^{\alpha\beta}g^{\lambda\mu}\right)$$

$$D^{\alpha\beta} \stackrel{\text{def}}{=} \frac{2E}{1+v}g^{\alpha\beta}$$

Note that the e_{33} component of the strain tensors does not appear because of assumption A-2. The linear form $F^{(3D)}$ represents the virtual work of external forces and reads

$$F^{(3D)}(\mathbf{V}) \stackrel{\text{def}}{=} \int_{\Lambda_t} \mathbf{F}\cdot\mathbf{V}\,\mathrm{d}V$$

where $\mathbf{F}$ denotes the applied body forces.

Equation (5) characterizes the solution of this 3D-elasticity problem for a body that is contained within the same geometrical bounds as the shell that we want to consider. The displacements $\mathbf{U}$ and $\mathbf{V}$ above are general 3D displacement vectors defined over the domain Λ_t (they must, of course, satisfy some boundary conditions). Clearly, a general shell element procedure does not really approximate the solution of the 3D problem, i.e. we do not expect that, when h (a parameter characteristic of the mesh size) tends to zero, the solution of the finite element procedure converges to the solution of Equation (5). Instead, a good candidate problem for the limit of the finite element solution is obtained by enforcing the kinematical assumption stated in assumption A-1 above in the whole domain (and not only at nodes). We therefore introduce in Equation (5) the assumption that $\mathbf{U}$ and $\mathbf{V}$ have the special form

$$\mathbf{U}(\xi_1,\xi_2,\xi_3) = \mathbf{u}(\xi_1,\xi_2) + \xi_3\theta_\lambda(\xi_1,\xi_2)\mathbf{a}^\lambda(\xi_1,\xi_2) \tag{6}$$

$$\mathbf{V}(\xi_1,\xi_2,\xi_3) = \mathbf{v}(\xi_1,\xi_2) + \xi_3\eta_\lambda(\xi_1,\xi_2)\mathbf{a}^\lambda(\xi_1,\xi_2) \tag{7}$$

The quantities θ_λ and η_λ are the covariant components of the first-order tensors $\underline{\boldsymbol{\theta}}$ and $\underline{\boldsymbol{\eta}}$. They are defined in the tangent plane and correspond to the rotations of fibres normal to the mid-surface in the original configuration. We get the modified variational formulation

$$A(\mathbf{u},\underline{\boldsymbol{\theta}};\mathbf{v},\underline{\boldsymbol{\eta}}) = F(\mathbf{v},\underline{\boldsymbol{\eta}}), \quad \forall(\mathbf{v},\underline{\boldsymbol{\eta}}) \tag{8}$$

where A and F are directly inferred from $A^{(3D)}$ and $F^{(3D)}$ by setting

$$A(\mathbf{u},\underline{\boldsymbol{\theta}};\mathbf{v},\underline{\boldsymbol{\eta}}) \stackrel{\text{def}}{=} A^{(3D)}(\mathbf{u}+\xi_3\theta_\lambda\mathbf{a}^\lambda;\mathbf{v}+\xi_3\eta_\lambda\mathbf{a}^\lambda)$$

$$F(\mathbf{v},\underline{\boldsymbol{\eta}}) \stackrel{\text{def}}{=} F^{(3D)}(\mathbf{v}+\xi_3\eta_\lambda\mathbf{a}^\lambda)$$

Although the integrals involved in A and F are three-dimensional, Equation (8) characterizes a two-dimensional (2D) problem since the variational unknowns and test functions are defined on the mid-surface only. We call this problem *the underlying 2D shell model*. Indeed, the dependence on the ξ_3-variable of all the terms under the integral signs can be made fully explicit. In particular,

we have

$$e_{\alpha\beta}(\mathbf{v}+\xi_3\eta_\lambda\mathbf{a}^\lambda)=\gamma_{\alpha\beta}(\mathbf{v})+\xi_3\chi_{\alpha\beta}(\mathbf{v},\underline{\boldsymbol{\eta}})-\xi_3^2\kappa_{\alpha\beta}(\underline{\boldsymbol{\eta}}) \tag{9}$$

$$e_{\alpha 3}(\mathbf{v}+\xi_3\eta_\lambda\mathbf{a}^\lambda)=\zeta_\alpha(\mathbf{v},\underline{\boldsymbol{\eta}}) \tag{10}$$

where

$$\gamma_{\alpha\beta}(\mathbf{v}) \stackrel{\text{def}}{=} \tfrac{1}{2}(v_{\alpha|\beta}+v_{\beta|\alpha})-b_{\alpha\beta}v_3$$

$$\chi_{\alpha\beta}(\mathbf{v},\underline{\boldsymbol{\eta}}) \stackrel{\text{def}}{=} \tfrac{1}{2}(\eta_{\alpha|\beta}+\eta_{\beta|\alpha}-b^\lambda_\beta v_{\lambda|\alpha}-b^\lambda_\alpha v_{\lambda|\beta})+c_{\alpha\beta}v_3$$

$$\kappa_{\alpha\beta}(\underline{\boldsymbol{\eta}}) \stackrel{\text{def}}{=} \tfrac{1}{2}(b^\lambda_\beta\eta_{\lambda|\alpha}+b^\lambda_\alpha\eta_{\lambda|\beta})$$

$$\zeta_\alpha(\mathbf{v},\underline{\boldsymbol{\eta}}) \stackrel{\text{def}}{=} \tfrac{1}{2}(\eta_\alpha+v_{3,\alpha}+b^\lambda_\alpha v_\lambda)$$

Note that the terms $\gamma_{\alpha\beta}$, $\chi_{\alpha\beta}$ and ζ_α are, respectively, the components of the classical membrane, bending and shear strain tensors that appear in the Naghdi shell model [10]. Also, the unknowns involved in the underlying model are the same—namely, a displacement vector and a rotation tensor—as in the Naghdi model. However, the underlying model is clearly different from the Naghdi model, and it is also different from shell models obtained by truncating Taylor expansions of the three-dimensional formulation (see, e.g., Reference [11]).

4. ANALYSIS OF THE UNDERLYING MODEL

We first need to recast Problem (8) in a rigorous mathematical context. We suppose that the shell is fully clamped on a part of its lateral boundary given by $\boldsymbol{\Phi}(\Gamma_0\times[-t/2,t/2])$ where Γ_0 is a part of $\partial\Omega$. We define the space of admissible 'displacements' by

$$\mathscr{U} \stackrel{\text{def}}{=} \{(\mathbf{v},\underline{\boldsymbol{\eta}})\in[H^1(\Omega)]^3\times[H^1(\Omega)]^2 \mid \mathbf{v}|_{\Gamma_0}\equiv\mathbf{0},\ \underline{\boldsymbol{\eta}}|_{\Gamma_0}\equiv\underline{\mathbf{0}}\}$$

Then the following proposition shows that Problem (8) is well-posed on $\mathscr{U}$ (see the appendix for the proof).

Proposition 4.1. Suppose $\mathbf{F}\in L^2(\Lambda_t)$. *There exists a unique* $(\mathbf{u},\underline{\boldsymbol{\theta}})$ *in* $\mathscr{U}$ *such that Equation (8) is satisfied for any* $(\mathbf{v},\underline{\boldsymbol{\eta}})$ *in* $\mathscr{U}$. *Furthermore, we have*

$$\|\mathbf{u},\underline{\boldsymbol{\theta}}\|_1\leqslant C\|\mathbf{F}\|_0 \tag{11}$$

We now want to perform the asymptotic analysis of the underlying model, i.e. the analysis of the behaviour of the solution of Problem (8) when the thickness parameter t becomes very small (and in the limit approaches zero). To that purpose, we need to make some assumptions on the loading. In particular, the applied body force must be scaled by some power of t in order for the solution of the problem to remain both bounded and non-vanishing when t tends to zero.

Therefore, we suppose

$$\mathbf{F} = t^{\rho}\mathbf{L} \tag{12}$$

where $\mathbf{L}$ is a 'force field' *independent of* t. The quantity t^{ρ} can be seen as the relevant order of magnitude of body forces that can be applied to the shell. The choice of ρ is addressed below. Furthermore, we suppose that $\mathbf{L}$ is smooth enough to have

$$\mathbf{L}(\xi_1, \xi_2, \xi_3) = \mathbf{l}_0(\xi_1, \xi_2) + \xi_3 \mathbf{l}_1(\xi_1, \xi_2) + \xi_3^2 \mathbf{B}(\xi_1, \xi_2, \xi_3) \tag{13}$$

where $\mathbf{l}_0$ and $\mathbf{l}_1$ are in $L^2(\Omega)$, while $\mathbf{B}$ is a bounded function.

Like for the Naghdi model, we now introduce the subspace of 'pure bending displacements':

$$\mathscr{U}_0 \stackrel{\text{def}}{=} \{(\mathbf{v}, \underline{\boldsymbol{\eta}}) \in \mathscr{U} \mid \gamma_{\alpha\beta}(\mathbf{v}) \equiv 0,\ \alpha, \beta = 1, 2,\ \ \zeta_{\alpha}(\mathbf{v}, \underline{\boldsymbol{\eta}}) \equiv 0,\ \alpha = 1, 2\}$$

and we say that pure bending is inhibited if

$$\mathscr{U}_0 = \{(\mathbf{0}, \underline{\mathbf{0}})\} \tag{14}$$

We proceed to demonstrate that the asymptotic behaviour of the underlying model is similar to that of the Naghdi model. We recall the bilinear forms which appear in the Naghdi formulation:

$$A^{(\mathrm{m+s})}(\mathbf{u}, \underline{\boldsymbol{\theta}}; \mathbf{v}, \underline{\boldsymbol{\eta}}) \stackrel{\text{def}}{=} \int_{\Omega} [\check{C}^{\alpha\beta\lambda\mu} \gamma_{\alpha\beta}(\mathbf{u}) \gamma_{\lambda\mu}(\mathbf{v}) + \check{D}^{\alpha\beta} \zeta_{\alpha}(\mathbf{u}, \underline{\boldsymbol{\theta}}) \zeta_{\beta}(\mathbf{v}, \underline{\boldsymbol{\eta}})] \, \mathrm{d}S$$

with the membrane and shear strain terms, where

$$\check{C}^{\alpha\beta\lambda\mu} \stackrel{\text{def}}{=} \frac{E}{2(1+\nu)} \left(a^{\alpha\lambda} a^{\beta\mu} + a^{\alpha\mu} a^{\beta\lambda} + \frac{2\nu}{1-\nu} a^{\alpha\beta} a^{\lambda\mu} \right)$$

$$\check{D}^{\alpha\beta} \stackrel{\text{def}}{=} \frac{2E}{1+\nu} a^{\alpha\beta}$$

and

$$A^{(\mathrm{b})}(\mathbf{u}, \underline{\boldsymbol{\theta}}; \mathbf{v}, \underline{\boldsymbol{\eta}}) \stackrel{\text{def}}{=} \frac{1}{12} \int_{\Omega} \check{C}^{\alpha\beta\lambda\mu} \chi_{\alpha\beta}(\mathbf{u}, \underline{\boldsymbol{\theta}}) \chi_{\lambda\mu}(\mathbf{v}, \underline{\boldsymbol{\eta}}) \, \mathrm{d}S$$

which contains the bending strains.

4.1. The case of non-inhibited pure bending

We suppose that $\mathscr{U}_0$ contains non-zero elements. Then, as is justified by the convergence result below, the appropriate scaling of the force is obtained by setting $\rho = 2$. The problem sequence in consideration is then

Find $(\mathbf{u}^{(t)}, \underline{\boldsymbol{\theta}}^{(t)})$ *in* $\mathscr{U}$ *such that, for all* $(\mathbf{v}, \underline{\boldsymbol{\eta}})$ *in* $\mathscr{U}$,

$$A(\mathbf{u}^{(t)}, \underline{\boldsymbol{\theta}}^{(t)}; \mathbf{v}, \underline{\boldsymbol{\eta}}) = t^2 \int_{\Lambda_t} \mathbf{L} \cdot (\mathbf{v} + \xi_3 \eta_{\lambda} \mathbf{a}^{\lambda}) \, \mathrm{d}V \tag{15}$$

We now introduce a problem posed in the subspace $\mathscr{U}_0$.

Find $(\mathbf{u}^{(0)}, \underline{\boldsymbol{\theta}}^{(0)})$ *in* $\mathscr{U}_0$ *such that, for all* $(\mathbf{v}, \underline{\boldsymbol{\eta}})$ in $\mathscr{U}_0$,

$$A^{(\mathrm{b})}(\mathbf{u}^{(0)}, \underline{\boldsymbol{\theta}}^{(0)}; \mathbf{v}, \underline{\boldsymbol{\eta}}) = \int_{\Omega} \mathbf{l}_0 \cdot \mathbf{v} \, \mathrm{d}S \tag{16}$$

We can then show the following convergence result (see the appendix).

Proposition 4.2. When t tends to zero, $(\mathbf{u}^{(t)}, \underline{\boldsymbol{\theta}}^{(t)})$*, the solution of (15) converges to* $(\mathbf{u}^{(0)}, \underline{\boldsymbol{\theta}}^{(0)})$*, the solution of (16), for the norm of* $\mathscr{U}$.

4.2. The case of inhibited pure bending

We now suppose that pure bending is inhibited. In this case, the relevant scaling corresponds to $\rho = 0$. The problem sequence is thus
Find $(\mathbf{u}^{(t)}, \underline{\boldsymbol{\theta}}^{(t)})$ *in* $\mathscr{U}$ *such that, for all* $(\mathbf{v}, \underline{\boldsymbol{\eta}})$ *in* $\mathscr{U}$,

$$A(\mathbf{u}^{(t)}, \underline{\boldsymbol{\theta}}^{(t)}; \mathbf{v}, \underline{\boldsymbol{\eta}}) = \int_{\Lambda_t} \mathbf{L} \cdot (\mathbf{v} + \xi_3 \eta_\lambda \mathbf{a}^\lambda) \, \mathrm{d}V \tag{17}$$

For the limit problem, we need to define the norm obtained from the membrane and shear energy terms of the Naghdi formulation:

$$\|\mathbf{v}, \underline{\boldsymbol{\eta}}\|_{(\mathrm{m+s})} \stackrel{\mathrm{def}}{=} [A^{(\mathrm{m+s})}(\mathbf{v}, \underline{\boldsymbol{\eta}}; \mathbf{v}, \underline{\boldsymbol{\eta}})]^{1/2}$$

and we define $\mathscr{V}$ as the space obtained by completion of $\mathscr{U}$ by this norm. We then introduce a variational problem posed on $\mathscr{V}$:
Find $(\mathbf{u}^{(\mathrm{l})}, \underline{\boldsymbol{\theta}}^{(\mathrm{l})})$ *in* $\mathscr{V}$ *such that, for all* $(\mathbf{v}, \underline{\boldsymbol{\eta}})$ *in* $\mathscr{V}$,

$$A^{(\mathrm{m+s})}(\mathbf{u}^{(\mathrm{l})}, \underline{\boldsymbol{\theta}}^{(\mathrm{l})}; \mathbf{v}, \underline{\boldsymbol{\eta}}) = \int_{\Omega} \mathbf{l}_0 \cdot \mathbf{v} \, \mathrm{d}S \tag{18}$$

and we have the following convergence result (see the appendix).

Proposition 4.3. Suppose $\mathbf{l}_0$ *is in* $\mathscr{V}'$*, the dual space of* $\mathscr{V}$*. Then, when t tends to zero,* $(\mathbf{u}^{(t)}, \underline{\boldsymbol{\theta}}^{(t)})$*, the solution of (17), converges to* $(\mathbf{u}^{(\mathrm{l})}, \underline{\boldsymbol{\theta}}^{(\mathrm{l})})$*, the solution of (18), for the norm* $\|\cdot\|_{(\mathrm{m+s})}$.

4.3. Conclusions on the asymptotic analysis

We conclude that the underlying 2D-model of the general shell finite element formulation displays the same asymptotic behaviour as the following Naghdi shell problem:

$$tA^{(\mathrm{m+s})}(\mathbf{u}^{(t)}, \underline{\boldsymbol{\theta}}^{(t)}; \mathbf{v}, \underline{\boldsymbol{\eta}}) + t^3 A^{(\mathrm{b})}(\mathbf{u}^{(t)}, \underline{\boldsymbol{\theta}}^{(t)}; \mathbf{v}, \underline{\boldsymbol{\eta}}) = t^{\rho+1} \int_{\Omega} \mathbf{l}_0 \cdot \mathbf{v} \, \mathrm{d}S \tag{19}$$

Note that the surface load of the Naghdi problem is set as the integral over the thickness of the first term of the Taylor expansion of the body forces.

Hence, the solution of the underlying 2D-model (Equation (8), with the loading set as in (12)) converges to the same limit solutions as problem (19) when the thickness parameter t tends to zero, with the same subspace of pure bending displacements that determines the asymptotic behaviour. Namely, when pure bending is not inhibited, the solution converges to the solution of the bending

problem as defined in (16). By contrast, when pure bending is inhibited, the solution converges to that of the membrane problem (18), provided that the loading satisfies the condition $\mathbf{l}_0 \in \mathscr{V}'$ (see Reference [5] for more details on this condition). It is the geometry of the mid-surface and the boundary conditions that decide whether or not pure bending is inhibited, hence into which category the shell falls. This issue is discussed in Reference [5].

Note also that, as a consequence, the underlying model is asymptotically equivalent to the model of linear three-dimensional elasticity, since this model features asymptotic behaviours similar to those of the Naghdi model when the thickness tends to zero (see Reference [12] and the references therein).

5. CONVERGENCE OF THE GENERAL SHELL ELEMENT DISCRETIZATION

The aim of this section is to show that the solution of the 'general shell element' procedure converges to the solution of the underlying 2D-model when the mesh is refined.

We consider a 2D-mesh defined on the midsurface by a set of nodes, elements, and shape functions (corresponding to Lagrange degrees of freedom). We call h the largest diameter of all elements in the mesh. According to Section 3, a general shell element procedure amounts to solving

$$\tilde{A}^{(3D)}(\mathbf{U}_h; \mathbf{V}) = \tilde{F}^{(3D)}(\mathbf{V}), \quad \forall \mathbf{V} \tag{20}$$

where $\mathbf{U}_h$ and $\mathbf{V}$ have the special form, on each element $\mathscr{E}$ of the mesh

$$\mathbf{U}_h = \sum_i \lambda_i(\xi_1, \xi_2)(\mathbf{u}_h^{(i)} + \xi_3 \boldsymbol{\tau}_h^{(i)}) \tag{21}$$

$$\mathbf{V} = \sum_i \lambda_i(\xi_1, \xi_2)(\mathbf{v}^{(i)} + \xi_3 \boldsymbol{\psi}^{(i)}) \tag{22}$$

Here, λ_i denotes the shape function attached to the ith node of the element, $\mathbf{u}_h^{(i)}$ and $\mathbf{v}^{(i)}$ the nodal displacements, and $\boldsymbol{\tau}_h^{(i)}$ and $\boldsymbol{\psi}^{(i)}$ the nodal rotations (i.e. vectors tangent to the mid-surface). In addition, the tilde symbol in $\tilde{A}^{(3D)}$ and in $\tilde{F}^{(3D)}$ means that all the geometric quantities involved are computed from the isoparametric approximation of the geometry

$$\tilde{\boldsymbol{\Phi}}(\xi_1, \xi_2, \xi_3)|_{\mathscr{E}} = \sum_i \lambda_i(\xi_1, \xi_2)(\boldsymbol{\phi}^{(i)} + \xi_3 \mathbf{a}_3^{(i)}) \tag{23}$$

where $\boldsymbol{\phi}^{(i)}$ and $\mathbf{a}_3^{(i)}$, respectively, denote the position of the mid-surface and the unit normal vector at node i. Namely,

$$\tilde{\boldsymbol{\Phi}} = \mathscr{I}(\boldsymbol{\phi}) + \xi_3 \mathscr{I}(\mathbf{a}_3) \tag{24}$$

where $\mathscr{I}$ denotes the interpolation operator (in Ω) corresponding to the finite element method considered. Note that we assume that $\mathbf{a}_3$ is known exactly at all nodes and is not obtained from the isoparametric approximation of the mid-surface geometry.

In order to establish the connection between the general shell element procedure and the underlying 2D-model, we first note that the formulation of the latter is equivalent to finding $(\mathbf{u}, \boldsymbol{\tau})$ in the space

$$\hat{\mathscr{U}} \overset{\text{def}}{=} \{(\mathbf{v}, \boldsymbol{\psi}) \in [H^1(\Omega)]^6 \mid \boldsymbol{\psi} \cdot \mathbf{a}_3 \equiv 0, \ \mathbf{v}|_{\Gamma_0} \equiv \mathbf{0}, \ \boldsymbol{\psi}|_{\Gamma_0} \equiv \mathbf{0}\}$$

such that, for all $(\mathbf{v}, \boldsymbol{\psi})$ in $\hat{\mathscr{U}}$,

$$\hat{A}(\mathbf{u}, \boldsymbol{\tau}; \mathbf{v}, \boldsymbol{\psi}) = \hat{F}(\mathbf{v}, \boldsymbol{\psi}) \tag{25}$$

where

$$\hat{A}(\mathbf{u}, \boldsymbol{\tau}; \mathbf{v}, \boldsymbol{\psi}) \overset{\text{def}}{=} A^{(3D)}(\mathbf{u} + \xi_3 \boldsymbol{\tau}; \mathbf{v} + \xi_3 \boldsymbol{\psi})$$

$$\hat{F}(\mathbf{v}, \boldsymbol{\psi}) \overset{\text{def}}{=} F^{(3D)}(\mathbf{v} + \xi_3 \boldsymbol{\psi})$$

The equivalence between (8) and (25) is indeed straightforward by the relations

$$\boldsymbol{\tau} = \theta_\lambda \mathbf{a}^\lambda \;\Leftrightarrow\; \theta_\lambda = \boldsymbol{\tau} \cdot \mathbf{a}_\lambda \tag{26}$$

We observe that definitions (21) and (22) are not compatible with (6) and (7), since the interpolation of vectors which are tangent to the mid-surface at the nodes is not tangent inside the elements. In order to still obtain a formulation of the finite element procedure as an *internal* approximation of the underlying 2D-model, we define the discrete space

$$\hat{\mathscr{U}}_h \overset{\text{def}}{=} \left\{ (\mathbf{v}, \boldsymbol{\psi}) \in \hat{\mathscr{U}} \mid \forall \mathscr{E},\ \mathbf{v}|_{\mathscr{E}} = \sum_i \lambda_i \mathbf{v}^{(i)}\ \ \boldsymbol{\psi}|_{\mathscr{E}} = \Pi \left[\sum_i \lambda_i \boldsymbol{\psi}^{(i)} \right],\ \ \boldsymbol{\psi}^{(i)} \cdot \mathbf{a}_3^{(i)} = 0 \right\}$$

where Π denotes the operator which projects a vector of $\mathbb{R}^3$ onto the plane tangent to the mid-surface. Note that, by definition,

$$\Pi \circ \mathscr{I}(\boldsymbol{\psi}) = \boldsymbol{\psi} \tag{27}$$

The general shell element procedure defined above can now be re-stated in the alternative manner: *Find* $(\mathbf{u}_h, \boldsymbol{\tau}_h) \in \hat{\mathscr{U}}_h$ *such that, for all* $(\mathbf{v}, \boldsymbol{\psi}) \in \hat{\mathscr{U}}_h$,

$$\hat{A}_h(\mathbf{u}_h, \boldsymbol{\tau}_h; \mathbf{v}, \boldsymbol{\psi}) = \hat{F}_h(\mathbf{v}, \boldsymbol{\psi}) \tag{28}$$

where

$$\hat{A}_h(\mathbf{u}_h, \boldsymbol{\tau}_h; \mathbf{v}, \boldsymbol{\psi}) \overset{\text{def}}{=} \hat{A}^{(3D)}(\mathbf{u}_h + \xi_3 \mathscr{I}(\boldsymbol{\tau}_h); \mathbf{v} + \xi_3 \mathscr{I}(\boldsymbol{\psi}))$$

$$\hat{F}_h(\mathbf{v}, \boldsymbol{\psi}) \overset{\text{def}}{=} \hat{F}^{(3D)}(\mathbf{v} + \xi_3 \mathscr{I}(\boldsymbol{\psi}))$$

In the form (28), we can see that the general shell element procedure is an approximation of (25) based on an approximate bilinear form $\hat{A}_h$ and an approximate linear form $\hat{F}_h$. Furthermore, comparing the definitions of $\hat{A}_h$ and $\hat{F}_h$ with those of $\hat{A}$ and $\hat{F}$, we observe that the consistency error for this approximation scheme has two sources: the approximation of the geometry and the presence of the interpolation operator. We now state our final result (see the appendix).

Proposition 5.1. Problem (28) has a unique solution. Furthermore, assuming that the solution of Problem (25) is smooth and that the mapping $\boldsymbol{\phi}$ *is also smooth, we have the following error estimate:*

$$\|\mathbf{u} - \mathbf{u}_h, \boldsymbol{\tau} - \boldsymbol{\tau}_h\|_1 \leqslant Ch \tag{29}$$

In Equation (29), C is a constant independent of the parameter h. This shows that the solution of the general shell element procedure converges to the solution of the underlying 2D-model.

6. GENERAL CONCLUSIONS

In this paper, we have shown that, although no shell model is explicitly used in the formulation of general shell elements [1, 4], we can construct a shell model by using the static and kinematic assumptions made in these finite element procedures. We called this model the underlying 2D-model.

This underlying 2D-model compares well with classical shell models since it can be shown to feature the same asymptotic behaviour as, for example, the Naghdi model when the thickness of the shell becomes very small.

Furthermore, the connection between the underlying 2D-model and the general shell elements was mathematically substantiated by establishing a convergence result of the finite element solution to the solution of the 2D-model.

The results given in the paper are valuable for the evaluation and design of improved shell finite element discretization schemes. At least two observations are important.

Firstly, the results show that numerical convergence studies of general shell element formulations can be designed using the Naghdi shell theory [5], but differences in the numerical results to closed-form Naghdi shell theory must be expected [6]. For shells that are not very thin, analytical solutions to the underlying mathematical model given in this paper should ideally be used in the convergence studies.

Secondly, the numerical and mathematical analyses of *mixed* shell element discretizations that are based on degenerating 3D continuum to shell behaviour should, ideally also, be conducted using the mathematical model established and analysed in this paper.

APPENDIX

From now on, we choose an upper bound $t_{\max}$ for the range of values of the thickness that we want to consider, such that

$$t_{\max} < 2 \inf_{(\xi_1,\xi_2)\in\bar{\Omega}} |R_{\min}(\xi_1, \xi_2)| \tag{A.1}$$

Lemma A.1. There exist two strictly positive constants c and C such that, for any $(\xi_1, \xi_2, \xi_3) \in \Lambda_{t_{\max}}$,

$$c\sqrt{a}(\xi_1, \xi_2) \leqslant \sqrt{g}(\xi_1, \xi_2, \xi_3) \leqslant C\sqrt{a}(\xi_1, \xi_2) \tag{A.2}$$

Proof. Directly inferred from

$$\sqrt{g} = \sqrt{a}(1 - 2H\xi_3 + K\xi_3^2) \tag{A.3}$$

and Equation (A.1). □

Lemma A.2. There exist two strictly positive constants c and C such that, for any $(\xi_1, \xi_2, \xi_3) \in \Lambda_{t_{\max}}$

$$ca^{\alpha\beta}(\xi_1, \xi_2) X_\alpha X_\beta \leqslant g^{\alpha\beta}(\xi_1, \xi_2, \xi_3) X_\alpha X_\beta \leqslant C\, a^{\alpha\beta}(\xi_1, \xi_2) X_\alpha X_\beta, \quad \forall (X_1, X_2) \in \mathbb{R}^2 \tag{A.4}$$

Proof. Consider the function

$$(X_1, X_2; \xi_1, \xi_2, \xi_3) \in \mathscr{C} \times \bar{\Lambda}_{t_{\max}} \mapsto \frac{g^{\alpha\beta}(\xi_1, \xi_2, \xi_3) X_\alpha X_\beta}{a^{\alpha\beta}(\xi_1, \xi_2) X_\alpha X_\beta}$$

where $\mathscr{C}$ is the unit circle of $\mathbb{R}^2$. This function is well defined (since the first fundamental form is positive definite over $\bar{\Omega}$) and clearly continuous. Therefore, since it is defined over a compact set, it admits a minimum and a maximum value that we denote by c and C, respectively. The minimum value (in particular) is reached, hence it is strictly positive because g is positive definite over $\bar{\Lambda}_{t_{\max}}$. Equation (A.4) follows with the same two constants c and C. □

Lemma A.3. There exist two strictly positive constants c and C such that, for any $(\xi_1, \xi_2, \xi_3) \in \Lambda_{t_{\max}}$

$$\begin{aligned} ca^{\alpha\lambda}(\xi_1, \xi_2) a^{\beta\mu}(\xi_1, \xi_2) Y_{\alpha\beta} Y_{\lambda\mu} &\leqslant g^{\alpha\lambda}(\xi_1, \xi_2, \xi_3) g^{\beta\mu}(\xi_1, \xi_2, \xi_3) Y_{\alpha\beta} Y_{\lambda\mu} \\ &\leqslant Ca^{\alpha\lambda}(\xi_1, \xi_2) a^{\beta\mu}(\xi_1, \xi_2) Y_{\alpha\beta} Y_{\lambda\mu}, \forall (Y_{11}, Y_{12}, Y_{21}, Y_{22}) \in \mathbb{R}^4 \end{aligned} \tag{A.5}$$

Proof. Similar to that of Lemma A.2. □

Lemma A.4. The bilinear form A is continuous and coercive over the space $\mathscr{U}$, *i.e. there exist two strictly positive constants c and C such that, for any* $(\mathbf{v}, \underline{\boldsymbol{\eta}})$ *in* $\mathscr{U}$,

$$c\|\mathbf{v}, \underline{\boldsymbol{\eta}}\|_1^2 \leqslant A(\mathbf{v}, \underline{\boldsymbol{\eta}}; \mathbf{v}, \underline{\boldsymbol{\eta}}) \leqslant C\|\mathbf{v}, \underline{\boldsymbol{\eta}}\|_1^2 \tag{A.6}$$

Proof. To make the notation shorter in this proof, we write e_{ij} instead of $e_{ij}(\mathbf{v} + \xi_3 \eta_\lambda \mathbf{a}^\lambda)$, and $\gamma_{\alpha\beta}$, $\chi_{\alpha\beta}$, $\kappa_{\alpha\beta}$ and ζ_α instead of $\gamma_{\alpha\beta}(\mathbf{v})$, $\chi_{\alpha\beta}(\mathbf{v}, \underline{\boldsymbol{\eta}})$, $\kappa_{\alpha\beta}(\underline{\boldsymbol{\eta}})$ and $\zeta_\alpha(\mathbf{v}, \underline{\boldsymbol{\eta}})$, respectively.

(i) *Coercivity*: Using Lemmas A.2 and A.3 we have

$$\begin{aligned} A(\mathbf{v}, \underline{\boldsymbol{\eta}}; \mathbf{v}, \underline{\boldsymbol{\eta}}) &\geqslant C \int_{\Lambda_t} [g^{\alpha\lambda} g^{\beta\mu} e_{\alpha\beta} e_{\lambda\mu} + g^{\alpha\beta} e_{\alpha 3} e_{\beta 3}]\, \mathrm{d}V \\ &\geqslant C \int_{\Lambda_t} [a^{\alpha\lambda} a^{\beta\mu} e_{\alpha\beta} e_{\lambda\mu} + a^{\alpha\beta} e_{\alpha 3} e_{\beta 3}]\, \mathrm{d}V \end{aligned} \tag{A.7}$$

since $g^{\alpha\beta} g^{\lambda\mu} e_{\alpha\beta} e_{\lambda\mu} = (g^{\alpha\beta} e_{\alpha\beta})^2 \geqslant 0$. We now use Equation (A.2) and integrate (A.7) through the thickness to obtain

$$A(\mathbf{v}, \underline{\boldsymbol{\eta}}; \mathbf{v}, \underline{\boldsymbol{\eta}}) \geqslant Ct \int_\Omega \left[a^{\alpha\lambda} a^{\beta\mu} \left(\gamma_{\alpha\beta}\gamma_{\lambda\mu} + \frac{t^2}{12} \chi_{\alpha\beta}\chi_{\lambda\mu} - \frac{t^2}{6} \gamma_{\alpha\beta}\kappa_{\lambda\mu} + \frac{t^4}{80} \kappa_{\alpha\beta}\kappa_{\lambda\mu} \right) + a^{\alpha\beta} \zeta_\alpha \zeta_\beta \right] \mathrm{d}S \tag{A.8}$$

Applying the Cauchy–Schwarz inequality on a symmetric positive-definite form, we have

$$\left| \frac{t^2}{6} a^{\alpha\lambda} a^{\beta\mu} \gamma_{\alpha\beta} \kappa_{\lambda\mu} \right| \leqslant \frac{1}{12} a^{\alpha\lambda} a^{\beta\mu} \left(\eta \gamma_{\alpha\beta}\gamma_{\lambda\mu} + \frac{t^4}{\eta} \kappa_{\alpha\beta}\kappa_{\lambda\mu} \right) \tag{A.9}$$

for any strictly positive η. Choosing $\eta = 10$, we obtain from (A.8)

$$A(\mathbf{v}, \underline{\boldsymbol{\eta}}; \mathbf{v}, \underline{\boldsymbol{\eta}}) \geqslant C \int_\Omega [a^{\alpha\lambda} a^{\beta\mu} (\gamma_{\alpha\beta}\gamma_{\lambda\mu} + \chi_{\alpha\beta}\chi_{\lambda\mu} + \kappa_{\alpha\beta}\kappa_{\lambda\mu}) + a^{\alpha\beta}\zeta_\alpha\zeta_\beta]\,\mathrm{d}S$$

$$\geqslant C \int_\Omega [a^{\alpha\lambda} a^{\beta\mu} (\gamma_{\alpha\beta}\gamma_{\lambda\mu} + \chi_{\alpha\beta}\chi_{\lambda\mu}) + a^{\alpha\beta}\zeta_\alpha\zeta_\beta]\,\mathrm{d}S \tag{A.10}$$

The coercivity now directly follows from that of the Naghdi model [3].

(ii) *Continuity*: Using a similar (although simpler) reasoning, we obtain

$$A(\mathbf{v}, \underline{\boldsymbol{\eta}}; \mathbf{v}, \underline{\boldsymbol{\eta}}) \leqslant C \int_\Omega [a^{\alpha\lambda} a^{\beta\mu} (\gamma_{\alpha\beta}\gamma_{\lambda\mu} + \chi_{\alpha\beta}\chi_{\lambda\mu} + \kappa_{\alpha\beta}\kappa_{\lambda\mu}) + a^{\alpha\beta}\zeta_\alpha\zeta_\beta]\,\mathrm{d}S \tag{A.11}$$

and the continuity follows from the boundedness of the geometric coefficients. □

Proof of Proposition 4.1. Since $\mathbf{F} \in L^2(\Lambda_t)$, using (A.2) we get

$$|F(\mathbf{v}, \underline{\boldsymbol{\eta}})| \leqslant C \|\mathbf{F}\|_{0,\Lambda_t} \|\mathbf{v}, \underline{\boldsymbol{\eta}}\|_0 \tag{A.12}$$

Hence, recalling (A.6), the variational problem is well-posed, i.e. there is a unique solution and Equation (11) holds. □

Proof of Proposition 4.2. We need to adapt the strategy used for standard penalized problems (see, e.g., Reference [13]). We divide our proof into 4 steps.

(i) *Uniform bound on the solution*: We start by noting that, in the proof of Lemma A.4, up to Equation (A.9) all constants are in fact independent of t. Therefore, we can obtain, instead of (A.10),

$$A(\mathbf{v}, \underline{\boldsymbol{\eta}}; \mathbf{v}, \underline{\boldsymbol{\eta}}) \geqslant Ct \int_\Omega [a^{\alpha\lambda} a^{\beta\mu} (\gamma_{\alpha\beta}\gamma_{\lambda\mu} + t^2\chi_{\alpha\beta}\chi_{\lambda\mu}) + a^{\alpha\beta}\zeta_\alpha\zeta_\beta]\,\mathrm{d}S \tag{A.13}$$

where C is independent of t. From now on, unless otherwise stated, all quantities denoted by C will be constants independent of t. Then,

$$A(\mathbf{v}, \underline{\boldsymbol{\eta}}; \mathbf{v}, \underline{\boldsymbol{\eta}}) \geqslant Ct^3 \int_\Omega \left[a^{\alpha\lambda} a^{\beta\mu} \left(\chi_{\alpha\beta}\chi_{\lambda\mu} + \frac{1}{t^2}\gamma_{\alpha\beta}\gamma_{\lambda\mu} \right) + \frac{1}{t^2} a^{\alpha\beta}\zeta_\alpha\zeta_\beta \right] \mathrm{d}S$$

$$\geqslant Ct^3 \int_\Omega \left[a^{\alpha\lambda} a^{\beta\mu} \left(\chi_{\alpha\beta}\chi_{\lambda\mu} + \frac{1}{t_{\max}^2}\gamma_{\alpha\beta}\gamma_{\lambda\mu} \right) + \frac{1}{t_{\max}^2} a^{\alpha\beta}\zeta_\alpha\zeta_\beta \right] \mathrm{d}S$$

$$\geqslant Ct^3 \|\mathbf{v}, \underline{\boldsymbol{\eta}}\|_1^2 \tag{A.14}$$

using again the coercivity of the Naghdi formulation.

On the other hand, using Equations (13) and (A.2), and integrating the right-hand side of (15) through the thickness, we have

$$\left| t^2 \int_{\Lambda_t} \mathbf{L} \cdot (\mathbf{v} + \xi_3 \eta_\lambda \mathbf{a}^\lambda)\,\mathrm{d}V \right| \leqslant Ct^3 (\|\mathbf{l}_0\|_0 \|\mathbf{v}\|_0 + t\|\mathbf{v}, \underline{\boldsymbol{\eta}}\|_0) \tag{A.15}$$

Hence, choosing $(\mathbf{v},\underline{\boldsymbol{\eta}})=(\mathbf{u}^{(t)},\underline{\boldsymbol{\theta}}^{(t)})$ in (15) and combining (A.14) and (A.15), we get the uniform bound

$$\|\mathbf{u}^{(t)},\underline{\boldsymbol{\theta}}^{(t)}\|_1 \leqslant C \tag{A.16}$$

(ii) *Weak convergence*: Since the sequence $(\mathbf{u}^{(t)},\underline{\boldsymbol{\theta}}^{(t)})$ is uniformly bounded, we can extract a subsequence that converges weakly to $(\mathbf{u}^{(\mathrm{w})},\underline{\boldsymbol{\theta}}^{(\mathrm{w})})$, an element of $\mathscr{U}$.

Let us rewrite the expression of A by using Equations (9) and (10), and making the change of variable $\xi_3=t\xi$. We get

$$\begin{aligned}
&A(\mathbf{u}^{(t)},\underline{\boldsymbol{\theta}}^{(t)};\mathbf{v},\underline{\boldsymbol{\eta}})\\
&\quad= t\int_{-1/2}^{1/2}\int_{\Omega}[C^{\alpha\beta\lambda\mu}(\gamma_{\alpha\beta}(\mathbf{u}^{(t)})+t\xi\chi_{\alpha\beta}(\mathbf{u}^{(t)},\underline{\boldsymbol{\theta}}^{(t)})-t^2\xi^2\kappa_{\alpha\beta}(\underline{\boldsymbol{\theta}}^{(t)}))\\
&\qquad\times(\gamma_{\lambda\mu}(\mathbf{v})+t\xi\chi_{\lambda\mu}(\mathbf{v},\underline{\boldsymbol{\eta}})-t^2\xi^2\kappa_{\lambda\mu}(\underline{\boldsymbol{\eta}}))\\
&\qquad+D^{\alpha\beta}\zeta_{\alpha}(\mathbf{u}^{(t)},\underline{\boldsymbol{\theta}}^{(t)})\zeta_{\beta}(\mathbf{v},\underline{\boldsymbol{\eta}})]\sqrt{g}\,\mathrm{d}\xi_1\,\mathrm{d}\xi_2\,\mathrm{d}\xi
\end{aligned} \tag{A.17}$$

Assuming sufficient smoothness of the midsurface, we can write Taylor expansions of all geometrically related quantities at $\xi_3=0$. In particular, in addition to Equation (A.3), we write

$$C^{\alpha\beta\lambda\mu}(\xi_1,\xi_2,\xi_3)=\check{C}^{\alpha\beta\lambda\mu}(\xi_1,\xi_2)+\xi_3\bar{C}^{\alpha\beta\lambda\mu}(\xi_1,\xi_2,\xi_3) \tag{A.18}$$

$$D^{\alpha\beta}(\xi_1,\xi_2,\xi_3)=\check{D}^{\alpha\beta}(\xi_1,\xi_2)+\xi_3\bar{D}^{\alpha\beta}(\xi_1,\xi_2,\xi_3) \tag{A.19}$$

where $\bar{C}^{\alpha\beta\lambda\mu}$ are $\bar{D}^{\alpha\beta}$ are bounded over $\bar{\Lambda}_{t_{\max}}$. Therefore, using the weak convergence of $(\mathbf{u}^{(t)},\underline{\boldsymbol{\theta}}^{(t)})$ to $(\mathbf{u}^{(\mathrm{w})},\underline{\boldsymbol{\theta}}^{(\mathrm{w})})$ and the uniform bound (A.16), we have

$$\frac{1}{t}A(\mathbf{u}^{(t)},\underline{\boldsymbol{\theta}}^{(t)};\mathbf{v},\underline{\boldsymbol{\eta}})\overset{t\to 0}{\longrightarrow}\int_{\Omega}[\check{C}^{\alpha\beta\lambda\mu}\gamma_{\alpha\beta}(\mathbf{u}^{(\mathrm{w})})\gamma_{\lambda\mu}(\mathbf{v})+\check{D}^{\alpha\beta}\zeta_{\alpha}(\mathbf{u}^{(\mathrm{w})},\underline{\boldsymbol{\theta}}^{(\mathrm{w})})\zeta_{\beta}(\mathbf{v},\underline{\boldsymbol{\eta}})]\sqrt{a}\,\mathrm{d}\xi_1\,\mathrm{d}\xi_2 \tag{A.20}$$

Then, since

$$\frac{1}{t}A(\mathbf{u}^{(t)},\underline{\boldsymbol{\theta}}^{(t)};\mathbf{v},\underline{\boldsymbol{\eta}})=t^2\int_{-1/2}^{1/2}\int_{\Omega}\mathbf{L}\cdot(\mathbf{v}+\xi_3\eta_{\lambda}\mathbf{a}^{\lambda})\sqrt{g}\,\mathrm{d}\xi_1\,\mathrm{d}\xi_2\,\mathrm{d}\xi\overset{t\to 0}{\longrightarrow}0 \tag{A.21}$$

we get

$$\int_{\Omega}[\check{C}^{\alpha\beta\lambda\mu}\gamma_{\alpha\beta}(\mathbf{u}^{(\mathrm{w})})\gamma_{\lambda\mu}(\mathbf{v})+\check{D}^{\alpha\beta}\zeta_{\alpha}(\mathbf{u}^{(\mathrm{w})},\underline{\boldsymbol{\theta}}^{(\mathrm{w})})\zeta_{\beta}(\mathbf{v},\underline{\boldsymbol{\eta}})]\sqrt{a}\,\mathrm{d}\xi_1\,\mathrm{d}\xi_2=0,\quad\forall(\mathbf{v},\underline{\boldsymbol{\eta}})\in\mathscr{U} \tag{A.22}$$

so that, choosing $(\mathbf{v},\underline{\boldsymbol{\eta}})=(\mathbf{u}^{(\mathrm{w})},\underline{\boldsymbol{\theta}}^{(\mathrm{w})})$, we infer

$$\sum_{\alpha,\beta}\|\gamma_{\alpha\beta}(\mathbf{u}^{(\mathrm{w})})\|_{0,\Omega}^2+\sum_{\alpha}\|\zeta_{\alpha}(\mathbf{u}^{(\mathrm{w})},\underline{\boldsymbol{\theta}}^{(\mathrm{w})})\|_{0,\Omega}^2=0 \tag{A.23}$$

Hence, we have proved that $(\mathbf{u}^{(\mathrm{w})},\underline{\boldsymbol{\theta}}^{(\mathrm{w})})\in\mathscr{U}_0$.

(iii) *Characterization of* $(\mathbf{u}^{(\mathrm{w})}, \underline{\boldsymbol{\theta}}^{(\mathrm{w})})$: We now take $(\mathbf{v}, \underline{\boldsymbol{\eta}}) \in \mathscr{U}_0$. According to Equation (A.17), we have

$$\frac{1}{t^3} A(\mathbf{u}^{(t)}, \underline{\boldsymbol{\theta}}^{(t)}; \mathbf{v}, \underline{\boldsymbol{\eta}}) = \frac{1}{t} \int_{-1/2}^{1/2} \int_{\Omega} C^{\alpha\beta\lambda\mu} (\gamma_{\alpha\beta}(\mathbf{u}^{(t)}) + t\xi\chi_{\alpha\beta}(\mathbf{u}^{(t)}, \underline{\boldsymbol{\theta}}^{(t)}) - t^2\xi^2\kappa_{\alpha\beta}(\underline{\boldsymbol{\theta}}^{(t)}))$$

$$\times (\xi\chi_{\lambda\mu}(\mathbf{v}, \underline{\boldsymbol{\eta}}) - t\xi^2\kappa_{\lambda\mu}(\underline{\boldsymbol{\eta}}))\sqrt{g}\, \mathrm{d}\xi_1\, \mathrm{d}\xi_2\, \mathrm{d}\xi \tag{A.24}$$

We use the expansions in Equations (A.3), (A.18) and (A.19) to develop this quantity in powers of t. The only term in $1/t$ is

$$\frac{1}{t} \int_{-1/2}^{1/2} \int_{\Omega} \xi \check{C}^{\alpha\beta\lambda\mu} \gamma_{\alpha\beta}(\mathbf{u}^{(t)}) \chi_{\lambda\mu}(\mathbf{v}, \underline{\boldsymbol{\eta}}) \sqrt{a}\, \mathrm{d}\xi_1\, \mathrm{d}\xi_2\, \mathrm{d}\xi$$

which is zero because of the integration on ξ. Next, all zero-order terms containing $\gamma_{\alpha\beta}(\mathbf{u}^{(t)})$ tend to zero when t tends to zero, because $\mathbf{u}^{(t)}$ converges weakly to $\mathbf{u}^{(\mathrm{w})}$ which is in $\mathscr{U}_0$. The only zero-order term without $\gamma_{\alpha\beta}(\mathbf{u}^{(t)})$ is

$$\int_{-1/2}^{1/2} \int_{\Omega} \xi^2 \check{C}^{\alpha\beta\lambda\mu} \chi_{\alpha\beta}(\mathbf{u}^{(t)}, \underline{\boldsymbol{\theta}}^{(t)}) \chi_{\lambda\mu}(\mathbf{v}, \underline{\boldsymbol{\eta}}) \sqrt{a}\, \mathrm{d}\xi_1\, \mathrm{d}\xi_2\, \mathrm{d}\xi$$

$$= \frac{1}{12} \int_{\Omega} \check{C}^{\alpha\beta\lambda\mu} \chi_{\alpha\beta}(\mathbf{u}^{(t)}, \underline{\boldsymbol{\theta}}^{(t)}) \chi_{\lambda\mu}(\mathbf{v}, \underline{\boldsymbol{\eta}}) \sqrt{a}\, \mathrm{d}\xi_1\, \mathrm{d}\xi_2 = A^{(\mathrm{b})}(\mathbf{u}^{(t)}, \underline{\boldsymbol{\theta}}^{(t)}; \mathbf{v}, \underline{\boldsymbol{\eta}}) \tag{A.25}$$

and, of course, all higher-order terms tend to zero with t. Therefore,

$$\frac{1}{t^3} A(\mathbf{u}^{(t)}, \underline{\boldsymbol{\theta}}^{(t)}; \mathbf{v}, \underline{\boldsymbol{\eta}}) \xrightarrow{t \to 0} A^{(\mathrm{b})}(\mathbf{u}^{(\mathrm{w})}, \underline{\boldsymbol{\theta}}^{(\mathrm{w})}; \mathbf{v}, \underline{\boldsymbol{\eta}}) \tag{A.26}$$

Furthermore, using Equations (13) and (A.3), we obtain

$$\frac{1}{t} \int_{\Lambda_t} \mathbf{L} \cdot (\mathbf{v} + \xi_3 \eta_i \mathbf{a}^{\lambda})\, \mathrm{d}V \xrightarrow{t \to 0} \int_{\Omega} \mathbf{l}_0 \cdot \mathbf{v}\, \mathrm{d}S \tag{A.27}$$

Hence, combining (A.26) and (A.27), we have shown that $(\mathbf{u}^{(\mathrm{w})}, \underline{\boldsymbol{\theta}}^{(\mathrm{w})})$ satisfies

$$A^{(\mathrm{b})}(\mathbf{u}^{(\mathrm{w})}, \underline{\boldsymbol{\theta}}^{(\mathrm{w})}; \mathbf{v}, \underline{\boldsymbol{\eta}}) = \int_{\Omega} \mathbf{l}_0 \cdot \mathbf{v}\, \mathrm{d}S \tag{A.28}$$

for any $(\mathbf{v}, \underline{\boldsymbol{\eta}})$ in $\mathscr{U}_0$. Therefore,

$$(\mathbf{u}^{(\mathrm{w})}, \underline{\boldsymbol{\theta}}^{(\mathrm{w})}) = (\mathbf{u}^{(0)}, \underline{\boldsymbol{\theta}}^{(0)}) \tag{A.29}$$

and, of course, the whole sequence $(\mathbf{u}^{(t)}, \underline{\boldsymbol{\theta}}^{(t)})$ converges weakly to $(\mathbf{u}^{(0)}, \underline{\boldsymbol{\theta}}^{(0)})$ in $\mathscr{U}$.

(iv) *Strong convergence*: Using Equation (A.14), we have

$$\begin{aligned}\|\mathbf{u}^{(t)}-\mathbf{u}^{(0)},\underline{\boldsymbol{\theta}}^{(t)}-\underline{\boldsymbol{\theta}}^{(0)}\|_1^2 &\leqslant \frac{C}{t^3}A(\mathbf{u}^{(t)}-\mathbf{u}^{(0)},\underline{\boldsymbol{\theta}}^{(t)}-\underline{\boldsymbol{\theta}}^{(0)};\mathbf{u}^{(t)}-\mathbf{u}^{(0)},\underline{\boldsymbol{\theta}}^{(t)}-\underline{\boldsymbol{\theta}}^{(0)})\\ &= \frac{C}{t^3}[A(\mathbf{u}^{(t)},\underline{\boldsymbol{\theta}}^{(t)};\mathbf{u}^{(t)}-\mathbf{u}^{(0)},\underline{\boldsymbol{\theta}}^{(t)}-\underline{\boldsymbol{\theta}}^{(0)})\\ &\quad -A(\mathbf{u}^{(0)},\underline{\boldsymbol{\theta}}^{(0)};\mathbf{u}^{(t)}-\mathbf{u}^{(0)},\underline{\boldsymbol{\theta}}^{(t)}-\underline{\boldsymbol{\theta}}^{(0)})]\end{aligned} \tag{A.30}$$

We first consider the second term on the right-hand side of this equation, i.e.

$$\mathrm{II}=\frac{1}{t^3}A(\mathbf{u}^{(0)},\underline{\boldsymbol{\theta}}^{(0)};\mathbf{u}^{(t)}-\mathbf{u}^{(0)},\underline{\boldsymbol{\theta}}^{(t)}-\underline{\boldsymbol{\theta}}^{(0)})$$

and we expand it in powers of t, using again Equations (A.3), (A.18) and (A.19). Since $(\mathbf{u}^{(0)},\underline{\boldsymbol{\theta}}^{(0)})$ is in $\mathscr{U}_0$, the expansion is similar to that performed in Step (iii). The only term in $1/t$ gives zero. Here, all the zero-order terms tend to zero because $(\mathbf{u}^{(t)}-\mathbf{u}^{(0)},\underline{\boldsymbol{\theta}}^{(t)}-\underline{\boldsymbol{\theta}}^{(0)})$ converges weakly to zero. Of course, all higher-order terms tend to zero also. Hence, II tends to zero.

We then treat the first term using the equilibrium equation (15). We get

$$I=\frac{1}{t^3}A(\mathbf{u}^{(t)},\underline{\boldsymbol{\theta}}^{(t)};\mathbf{u}^{(t)}-\mathbf{u}^{(0)},\underline{\boldsymbol{\theta}}^{(t)}-\underline{\boldsymbol{\theta}}^{(0)})=\frac{1}{t}\int_{\Lambda_t}\mathbf{L}\cdot[\mathbf{u}^{(t)}-\mathbf{u}^{(0)}+\xi_3(\theta_\lambda^{(t)}-\theta_\lambda^{(0)})\mathbf{a}^\lambda]\,\mathrm{d}V \tag{A.31}$$

Using Equations (13) and (A.3) to perform an expansion, it is again easy to see that all terms tend to zero.

Finally, from Equation (A.30), it follows that $\|\mathbf{u}^{(t)}-\mathbf{u}^{(0)},\underline{\boldsymbol{\theta}}^{(t)}-\underline{\boldsymbol{\theta}}^{(0)}\|_1$ tends to zero, hence $(\mathbf{u}^{(t)},\underline{\boldsymbol{\theta}}^{(t)})$ converges strongly to $(\mathbf{u}^{(0)},\underline{\boldsymbol{\theta}}^{(0)})$. □

Proof of Proposition 4.3. We follow and adapt the main steps of the classical proof of convergence for singular perturbation problems (see Reference [14]). We divide this proof into 3 parts.

(i) *Uniform bound on the solution*: We start like in the proof of Proposition 4.2 and, from (A.13), we directly infer

$$A(\mathbf{v},\underline{\boldsymbol{\eta}};\mathbf{v},\underline{\boldsymbol{\eta}})\geqslant Ct(\|\mathbf{v},\underline{\boldsymbol{\eta}}\|_{(\mathrm{m+s})}^2+t^2\|\mathbf{v},\underline{\boldsymbol{\eta}}\|_1^2) \tag{A.32}$$

On the other hand, using Equations (13) and (A.3), we perform an expansion of the right-hand side of (17) and we obtain

$$\int_{\Lambda_t}\mathbf{L}\cdot(\mathbf{v}+\xi_3\eta_\lambda\mathbf{a}^\lambda)\,\mathrm{d}V=t\int_\Omega\mathbf{l}_0\cdot\mathbf{v}\,\mathrm{d}S+R \tag{A.33}$$

where, since all first-order terms in ξ_3 vanish due to the integration through the thickness, the remainder R is bounded as

$$|R|\leqslant Ct^3\|\mathbf{v},\underline{\boldsymbol{\eta}}\|_0 \tag{A.34}$$

Hence, since $\mathbf{l}_0$ is in $\mathscr{V}'$ we have

$$\left|\int_{\Lambda_t}\mathbf{L}\cdot(\mathbf{v}+\xi_3\eta_\lambda\mathbf{a}^\lambda)\,\mathrm{d}V\right|\leqslant Ct(\|\mathbf{v},\underline{\boldsymbol{\eta}}\|_{(\mathrm{m+s})}+t^2\|\mathbf{v},\underline{\boldsymbol{\eta}}\|_0) \tag{A.35}$$

Then, taking $(\mathbf{v}, \underline{\boldsymbol{\eta}}) = (\mathbf{u}^{(t)}, \underline{\boldsymbol{\theta}}^{(t)})$ and combining Equations (17), (A.32) and (A.35), we get

$$\|\mathbf{u}^{(t)}, \underline{\boldsymbol{\theta}}^{(t)}\|_{(\mathrm{m+s})} + t\|\mathbf{u}^{(t)}, \underline{\boldsymbol{\theta}}^{(t)}\|_1 \leqslant C \tag{A.36}$$

(ii) *Weak convergence*: Since the sequence $(\mathbf{u}^{(t)}, \underline{\boldsymbol{\theta}}^{(t)})$ is uniformly bounded in the norms $\|\cdot\|_{(\mathrm{m+s})}$ and $t\|\cdot\|_1$, we can extract a subsequence that converges weakly in $\mathscr{V}$ to $(\mathbf{u}^{(\mathrm{w})}, \underline{\boldsymbol{\theta}}^{(\mathrm{w})})$. Of course this subsequence remains bounded in the norm $t\|\cdot\|_1$.

We now suppose that the geometry is sufficiently regular to allow a second-order Taylor expansion of the coefficients $C^{\alpha\beta\lambda\mu}$ and $D^{\alpha\beta}$, i.e.

$$C^{\alpha\beta\lambda\mu}(\xi_1, \xi_2, \xi_3) = \check{C}^{\alpha\beta\lambda\mu}(\xi_1, \xi_2) + \xi_3 \bar{C}^{\alpha\beta\lambda\mu}(\xi_1, \xi_2) + \xi_3^2 \hat{C}^{\alpha\beta\lambda\mu}(\xi_1, \xi_2, \xi_3) \tag{A.37}$$

$$D^{\alpha\beta}(\xi_1, \xi_2, \xi_3) = \check{D}^{\alpha\beta}(\xi_1, \xi_2) + \xi_3 \bar{D}^{\alpha\beta}(\xi_1, \xi_2) + \xi_3^2 \hat{D}^{\alpha\beta}(\xi_1, \xi_2, \xi_3) \tag{A.38}$$

where $\bar{C}^{\alpha\beta\lambda\mu}$ and $\bar{D}^{\alpha\beta}$ are bounded over $\bar{\Omega}$, while $\hat{C}^{\alpha\beta\lambda\mu}$ and $\hat{D}^{\alpha\beta}$ are bounded over $\bar{\Lambda}_{t_{\max}}$.

Using the same change of variable ($\xi_3 = t\xi$) as in Equation (A.17), then Equations (A.3), (A.37) and (A.38) to perform a Taylor expansion, we obtain

$$\frac{1}{t} A(\mathbf{u}^{(t)}, \underline{\boldsymbol{\theta}}^{(t)}; \mathbf{v}, \underline{\boldsymbol{\eta}}) = A^{(\mathrm{m+s})}(\mathbf{u}^{(t)}, \underline{\boldsymbol{\theta}}^{(t)}; \mathbf{v}, \underline{\boldsymbol{\eta}}) + R \tag{A.39}$$

with

$$|R| \leqslant Ct^2 \|\mathbf{u}^{(t)}, \underline{\boldsymbol{\theta}}^{(t)}\|_1 \|\mathbf{v}, \underline{\boldsymbol{\eta}}\|_1 \tag{A.40}$$

because, again, all the first-order terms of the expansion vanish with the integral through the thickness. Keeping $(\mathbf{v}, \underline{\boldsymbol{\eta}})$ fixed and making t tend to zero in (A.39), we have

$$A^{(\mathrm{m+s})}(\mathbf{u}^{(t)}, \underline{\boldsymbol{\theta}}^{(t)}; \mathbf{v}, \underline{\boldsymbol{\eta}}) \xrightarrow{t \to 0} A^{(\mathrm{m+s})}(\mathbf{u}^{(\mathrm{w})}, \underline{\boldsymbol{\theta}}^{(\mathrm{w})}; \mathbf{v}, \underline{\boldsymbol{\eta}}) \tag{A.41}$$

and R tends to zero since $t\|\mathbf{u}^{(t)}, \underline{\boldsymbol{\theta}}^{(t)}\|_1$ remains bounded in (A.40). Thus,

$$\frac{1}{t} A(\mathbf{u}^{(t)}, \underline{\boldsymbol{\theta}}^{(t)}; \mathbf{v}, \underline{\boldsymbol{\eta}}) \xrightarrow{t \to 0} A^{(\mathrm{m+s})}(\mathbf{u}^{(\mathrm{w})}, \underline{\boldsymbol{\theta}}^{(\mathrm{w})}; \mathbf{v}, \underline{\boldsymbol{\eta}}) \tag{A.42}$$

On the other hand, using (A.33) and (A.34) we have

$$\frac{1}{t} \int_{\Lambda_t} \mathbf{L} \cdot (\mathbf{v} + \xi_3 \eta_\lambda \mathbf{a}^\lambda) \, \mathrm{d}V \xrightarrow{t \to 0} \int_\Omega \mathbf{l}_0 \cdot \mathbf{v} \, \mathrm{d}S \tag{A.43}$$

Therefore, $(\mathbf{u}^{(\mathrm{w})}, \underline{\boldsymbol{\theta}}^{(\mathrm{w})})$ is the element of $\mathscr{V}$ that satisfies

$$A^{(\mathrm{m+s})}(\mathbf{u}^{(\mathrm{w})}, \underline{\boldsymbol{\theta}}^{(\mathrm{w})}; \mathbf{v}, \underline{\boldsymbol{\eta}}) = \int_\Omega \mathbf{l}_0 \cdot \mathbf{v} \, \mathrm{d}S \tag{A.44}$$

for any $(\mathbf{v}, \underline{\boldsymbol{\eta}})$ in $\mathscr{U}$. Hence

$$(\mathbf{u}^{(\mathrm{w})}, \underline{\boldsymbol{\theta}}^{(\mathrm{w})}) = (\mathbf{u}^{(\mathrm{l})}, \underline{\boldsymbol{\theta}}^{(\mathrm{l})}) \tag{A.45}$$

and we conclude that the whole sequence $(\mathbf{u}^{(t)}, \underline{\boldsymbol{\theta}}^{(t)})$ converges weakly to $(\mathbf{u}^{(\mathrm{l})}, \underline{\boldsymbol{\theta}}^{(\mathrm{l})})$.

(iii) *Strong convergence*: Define

$$\bar{A}^{(\mathrm{m+s})}(\mathbf{u},\underline{\boldsymbol{\theta}};\mathbf{v},\underline{\boldsymbol{\eta}})=\frac{1}{t}\int_{\Lambda_t}[C^{\alpha\beta\lambda\mu}\gamma_{\alpha\beta}(\mathbf{u})\gamma_{\lambda\mu}(\mathbf{v})+D^{\alpha\beta}\zeta_\alpha(\mathbf{u},\underline{\boldsymbol{\theta}})\zeta_\beta(\mathbf{v},\underline{\boldsymbol{\eta}})]\,\mathrm{d}V \tag{A.46}$$

The limit $(\mathbf{u}^{(\mathrm{l})},\underline{\boldsymbol{\theta}}^{(\mathrm{l})})$ is in $\mathscr{V}$, hence the limit membrane and shear deformation strains $\gamma_{\alpha\beta}(\mathbf{u}^{(\mathrm{l})})$ and $\zeta_\alpha(\mathbf{u}^{(\mathrm{l})},\underline{\boldsymbol{\theta}}^{(\mathrm{l})})$ are in $L^2(\Omega)$. Therefore, we can define the quantity

$$I=\bar{A}^{(\mathrm{m+s})}(\mathbf{u}^{(t)}-\mathbf{u}^{(\mathrm{l})},\underline{\boldsymbol{\theta}}^{(t)}-\underline{\boldsymbol{\theta}}^{(\mathrm{l})};\mathbf{u}^{(t)}-\mathbf{u}^{(\mathrm{l})},\underline{\boldsymbol{\theta}}^{(t)}-\underline{\boldsymbol{\theta}}^{(\mathrm{l})}) \tag{A.47}$$

and we have

$$I=A^{(\mathrm{m+s})}(\mathbf{u}^{(t)}-\mathbf{u}^{(\mathrm{l})},\underline{\boldsymbol{\theta}}^{(t)}-\underline{\boldsymbol{\theta}}^{(\mathrm{l})};\mathbf{u}^{(t)}-\mathbf{u}^{(\mathrm{l})},\underline{\boldsymbol{\theta}}^{(t)}-\underline{\boldsymbol{\theta}}^{(\mathrm{l})})+R \tag{A.48}$$

where R is the remainder of the Taylor expansion obtained by using Equations (A.3), (A.37) and (A.38). Of course, R tends to zero with t, hence $(\mathbf{u}^{(t)},\underline{\boldsymbol{\theta}}^{(t)})$ converges strongly in $\mathscr{V}$ to $(\mathbf{u}^{(\mathrm{l})},\underline{\boldsymbol{\theta}}^{(\mathrm{l})})$ if and only if I tends to zero, which we proceed to show.

We develop I into

$$I=\bar{A}^{(\mathrm{m+s})}(\mathbf{u}^{(t)},\underline{\boldsymbol{\theta}}^{(t)};\mathbf{u}^{(t)},\underline{\boldsymbol{\theta}}^{(t)})+\bar{A}^{(\mathrm{m+s})}(\mathbf{u}^{(\mathrm{l})},\underline{\boldsymbol{\theta}}^{(\mathrm{l})};\mathbf{u}^{(\mathrm{l})},\underline{\boldsymbol{\theta}}^{(\mathrm{l})})-2\bar{A}^{(\mathrm{m+s})}(\mathbf{u}^{(t)},\underline{\boldsymbol{\theta}}^{(t)};\mathbf{u}^{(\mathrm{l})},\underline{\boldsymbol{\theta}}^{(\mathrm{l})}) \tag{A.49}$$

Clearly,

$$\bar{A}^{(\mathrm{m+s})}(\mathbf{u}^{(\mathrm{l})},\underline{\boldsymbol{\theta}}^{(\mathrm{l})};\mathbf{u}^{(\mathrm{l})},\underline{\boldsymbol{\theta}}^{(\mathrm{l})})\xrightarrow{t\to 0}A^{(\mathrm{m+s})}(\mathbf{u}^{(\mathrm{l})},\underline{\boldsymbol{\theta}}^{(\mathrm{l})};\mathbf{u}^{(\mathrm{l})},\underline{\boldsymbol{\theta}}^{(\mathrm{l})})=\int_\Omega \mathbf{l}_0\cdot\mathbf{u}^{(\mathrm{l})}\,\mathrm{d}S \tag{A.50}$$

and, because of the weak convergence of $(\mathbf{u}^{(t)},\underline{\boldsymbol{\theta}}^{(t)})$, we also have

$$\bar{A}^{(\mathrm{m+s})}(\mathbf{u}^{(t)},\underline{\boldsymbol{\theta}}^{(t)};\mathbf{u}^{(\mathrm{l})},\underline{\boldsymbol{\theta}}^{(\mathrm{l})})\xrightarrow{t\to 0}A^{(\mathrm{m+s})}(\mathbf{u}^{(\mathrm{l})},\underline{\boldsymbol{\theta}}^{(\mathrm{l})};\mathbf{u}^{(\mathrm{l})},\underline{\boldsymbol{\theta}}^{(\mathrm{l})})=\int_\Omega \mathbf{l}_0\cdot\mathbf{u}^{(\mathrm{l})}\,\mathrm{d}S \tag{A.51}$$

We now focus on the first term of the right-hand side of Equation (A.49). Since it only concerns $(\mathbf{u}^{(t)},\underline{\boldsymbol{\theta}}^{(t)})$, we omit repeating it in the expression of the strains in the following derivation. We have

$$\begin{aligned}
&\bar{A}^{(\mathrm{m+s})}(\mathbf{u}^{(t)},\underline{\boldsymbol{\theta}}^{(t)};\mathbf{u}^{(t)},\underline{\boldsymbol{\theta}}^{(t)})\\
&\quad=\frac{1}{t}A(\mathbf{u}^{(t)},\underline{\boldsymbol{\theta}}^{(t)};\mathbf{u}^{(t)},\underline{\boldsymbol{\theta}}^{(t)})+\frac{1}{t}\int_{\Lambda_t}C^{\alpha\beta\lambda\mu}\gamma_{\alpha\beta}\gamma_{\lambda\mu}\,\mathrm{d}V\\
&\qquad-\frac{1}{t}\int_{\Lambda_t}C^{\alpha\beta\lambda\mu}(\gamma_{\alpha\beta}+\xi_3\chi_{\alpha\beta}-\xi_3^2\kappa_{\alpha\beta})(\gamma_{\lambda\mu}+\xi_3\chi_{\lambda\mu}-\xi_3^2\kappa_{\lambda\mu})\,\mathrm{d}V\\
&\quad=\frac{1}{t}\int_{\Lambda_t}\mathbf{L}\cdot(\mathbf{u}^{(t)}+\xi_3\theta_\lambda^{(t)}\mathbf{a}^\lambda)\,\mathrm{d}V-\frac{2}{t}\int_{\Lambda_t}C^{\alpha\beta\lambda\mu}\gamma_{\alpha\beta}(\xi_3\chi_{\lambda\mu}-\xi_3^2\kappa_{\lambda\mu})\,\mathrm{d}V\\
&\qquad-\frac{1}{t}\int_{\Lambda_t}C^{\alpha\beta\lambda\mu}(\xi_3\chi_{\alpha\beta}-\xi_3^2\kappa_{\alpha\beta})(\xi_3\chi_{\lambda\mu}-\xi_3^2\kappa_{\lambda\mu})\,\mathrm{d}V
\end{aligned} \tag{A.52}$$

From Equations (A.33) and (A.34), recalling that $(\mathbf{u}^{(t)}, \underline{\boldsymbol{\theta}}^{(t)})$ converges weakly to $(\mathbf{u}^{(1)}, \underline{\boldsymbol{\theta}}^{(1)})$ in $\mathscr{V}$, that $\mathbf{l}_0$ is in $\mathscr{V}'$ and that $t\|\mathbf{u}^{(t)}, \underline{\boldsymbol{\theta}}^{(t)}\|_1$ is bounded, we infer

$$\frac{1}{t}\int_{\Lambda_t} \mathbf{L}\cdot(\mathbf{u}^{(t)} + \xi_3\theta_\lambda^{(t)}\mathbf{a}^\lambda)\,\mathrm{d}V \xrightarrow{t\to 0} \int_\Omega \mathbf{l}_0\cdot\mathbf{u}^{(1)}\,\mathrm{d}S \tag{A.53}$$

For the second term of the right-hand side of (A.52), we perfom a Taylor expansion using (A.3) and (A.37). The first-order terms vanish and we get, by the Cauchy–Schwarz inequality,

$$\left|\frac{2}{t}\int_{\Lambda_t} C^{\alpha\beta\lambda\mu}\gamma_{\alpha\beta}(\xi_3\chi_{\lambda\mu} - \xi_3^2\kappa_{\lambda\mu})\,\mathrm{d}V\right| \leqslant Ct^2\left(\sum_{\alpha,\beta}\|\gamma_{\alpha\beta}\|_0\right)\|\mathbf{u}^{(t)}, \underline{\boldsymbol{\theta}}^{(t)}\|_1 \xrightarrow{t\to 0} 0 \tag{A.54}$$

since the membrane strains remain bounded in $L^2(\Omega)$ and $t\|\mathbf{u}^{(t)}, \underline{\boldsymbol{\theta}}^{(t)}\|_1$ is bounded.

Furthermore, we have

$$\frac{1}{t}\int_{\Lambda_t} C^{\alpha\beta\lambda\mu}(\xi_3\chi_{\alpha\beta} - \xi_3^2\kappa_{\alpha\beta})(\xi_3\chi_{\lambda\mu} - \xi_3^2\kappa_{\lambda\mu})\,\mathrm{d}V \geqslant 0 \tag{A.55}$$

since $C^{\alpha\beta\lambda\mu}$ defines a positive-definite bilinear form on second-order tensors.
Finally, combining Equations (A.49)–(A.55), we see that I is the sum of

(1) a group of terms with definite limits when t tends to zero, the combination of which yields zero;
(2) a negative term.

Since I is positive due to the positive-definite characters of $C^{\alpha\beta\lambda\mu}$ and $D^{\alpha\beta}$, it follows that I tends to zero with t, which proves the strong convergence result. □

We now proceed to establish the result stated in Proposition 5.1, i.e. we analyse the convergence of the finite element procedure when h tends to zero for a fixed t. In the forthcoming arguments, we thus allow bounding constants to incorporate a dependence on t. The following lemma is crucial for the consistency estimate.

Lemma A.5. Consider a continuous vector field $\boldsymbol{\psi}$ *tangent to the mid-surface at all points* (*i.e.* $\boldsymbol{\psi}\cdot\mathbf{a}_3 \equiv 0$), *and let* $\boldsymbol{\psi}_{\mathrm{int}}$ *be the vector field obtained by interpolating* $\boldsymbol{\psi}$ *using the finite element shape functions. Then*

$$\|\boldsymbol{\psi}_{\mathrm{int}}\cdot\mathbf{a}_3\|_1 \leqslant Ch\|\boldsymbol{\psi}_{\mathrm{int}}\|_1 \tag{A.56}$$

$$\|\boldsymbol{\psi}_{\mathrm{int}}\cdot\mathbf{a}_3\|_0 \leqslant Ch^2\|\boldsymbol{\psi}_{\mathrm{int}}\|_1 \tag{A.57}$$

Proof. We denote by $\mathscr{M}$ the 'piecewise-mean' operator. Namely, on each element $\mathscr{E}$,

$$\mathscr{M}(\boldsymbol{\psi})|_{\mathscr{E}} = \frac{1}{|\mathscr{E}|}\int_{\mathscr{E}}\boldsymbol{\psi}\,\mathrm{d}S$$

where $|\mathscr{E}|$ is the area of the surface comprised within $\mathscr{E}$.

Define now

$$\boldsymbol{\psi}_{\mathrm{m}} \overset{\mathrm{def}}{=} \Pi\circ\mathscr{M}(\boldsymbol{\psi}_{\mathrm{int}})$$

We have

$$\begin{aligned}\boldsymbol{\psi}_{\text{int}} \cdot \mathbf{a}_3 &= (\boldsymbol{\psi}_{\text{int}} - \boldsymbol{\psi}_{\text{m}}) \cdot \mathbf{a}_3 \\ &= (\boldsymbol{\psi}_{\text{int}} - \mathscr{I}(\boldsymbol{\psi}_{\text{m}})) \cdot \mathbf{a}_3 + (\mathscr{I}(\boldsymbol{\psi}_{\text{m}}) - \boldsymbol{\psi}_{\text{m}}) \cdot \mathbf{a}_3 \end{aligned} \tag{A.58}$$

We start by bounding the second term of the above right-hand side. Standard interpolation estimates give

$$\|\mathscr{I}(\boldsymbol{\psi}_{\text{m}}) - \boldsymbol{\psi}_{\text{m}}\|_{l,\mathscr{E}} \leqslant C h_{\mathscr{E}}^{k+1-l} |\boldsymbol{\psi}_{\text{m}}|_{k+1,\mathscr{E}}, \quad l = 0, 1 \tag{A.59}$$

where $h_{\mathscr{E}}$ is the diameter of element $\mathscr{E}$ and k is the order of approximation of the finite element shape functions. Furthermore, recalling that $\mathscr{M}(\boldsymbol{\psi}_{\text{int}})$ is constant over $\mathscr{E}$ and that, for any vector field $\mathbf{v}$

$$\Pi(\mathbf{v}) = \mathbf{v} - (\mathbf{v} \cdot \mathbf{a}_3)\mathbf{a}_3 \tag{A.60}$$

we have, assuming that the chart is sufficiently regular

$$|\boldsymbol{\psi}_{\text{m}}|_{k+1,\mathscr{E}} \leqslant C \sqrt{|\mathscr{E}|}\ \|\mathscr{M}(\boldsymbol{\psi}_{\text{int}})\| \tag{A.61}$$

By the Cauchy–Schwarz inequality, we have

$$\|\mathscr{M}(\boldsymbol{\psi}_{\text{int}})\| = \frac{1}{|\mathscr{E}|} \left\| \int_{\mathscr{E}} \boldsymbol{\psi}_{\text{int}}\, \mathrm{d}S \right\| \leqslant \frac{1}{\sqrt{|\mathscr{E}|}} \|\boldsymbol{\psi}_{\text{int}}\|_{0,\mathscr{E}} \tag{A.62}$$

Hence, combining (A.59)–(A.62), we obtain

$$\|(\mathscr{I}(\boldsymbol{\psi}_{\text{m}}) - \boldsymbol{\psi}_{\text{m}}) \cdot \mathbf{a}_3\|_{l,\mathscr{E}} \leqslant C h_{\mathscr{E}}^{k+1-l} \|\boldsymbol{\psi}_{\text{int}}\|_{0,\mathscr{E}}, \quad l = 0, 1 \tag{A.63}$$

We then focus on the first term of the right-hand side of Equation (A.58),

$$(\boldsymbol{\psi}_{\text{int}} - \mathscr{I}(\boldsymbol{\psi}_{\text{m}})) \cdot \mathbf{a}_3|_{\mathscr{E}} = \sum_i \lambda_i (\boldsymbol{\psi}_{\text{int}}^{(i)} - \boldsymbol{\psi}_{\text{m}}^{(i)}) \cdot \mathbf{a}_3 = \sum_i \lambda_i (\boldsymbol{\psi}_{\text{int}}^{(i)} - \boldsymbol{\psi}_{\text{m}}^{(i)}) \cdot (\mathbf{a}_3 - \mathbf{a}_3^{(i)}) \tag{A.64}$$

We tackle this expression by first bounding the Euclidean norm of $(\boldsymbol{\psi}_{\text{int}}^{(i)} - \boldsymbol{\psi}_{\text{m}}^{(i)})$. We write

$$\|\boldsymbol{\psi}_{\text{int}}^{(i)} - \boldsymbol{\psi}_{\text{m}}^{(i)}\| \leqslant \|\boldsymbol{\psi}_{\text{int}}^{(i)} - \mathscr{M}(\boldsymbol{\psi}_{\text{int}})\| + \|\mathscr{M}(\boldsymbol{\psi}_{\text{int}}) - \boldsymbol{\psi}_{\text{m}}^{(i)}\| \tag{A.65}$$

Using standard scaling arguments, we get

$$\sup_i \|\boldsymbol{\psi}_{\text{int}}^{(i)} - \mathscr{M}(\boldsymbol{\psi}_{\text{int}})\| \leqslant C |\boldsymbol{\psi}_{\text{int}}|_{1,\mathscr{E}} \tag{A.66}$$

For the second term of Equation (A.65), we have

$$\begin{aligned}\|\mathscr{M}(\boldsymbol{\psi}_{\text{int}}) - \boldsymbol{\psi}_{\text{m}}^{(i)}\| &= |\mathscr{M}(\boldsymbol{\psi}_{\text{int}}) \cdot \mathbf{a}_3^{(i)}| = \frac{1}{|\mathscr{E}|} \left| \int_{\mathscr{E}} \boldsymbol{\psi}_{\text{int}} \cdot \mathbf{a}_3^{(i)}\, \mathrm{d}S \right| \\ &\leqslant \frac{1}{|\mathscr{E}|} \left(\left| \int_{\mathscr{E}} \boldsymbol{\psi}_{\text{int}} \cdot \mathbf{a}_3\, \mathrm{d}S \right| + \left| \int_{\mathscr{E}} \boldsymbol{\psi}_{\text{int}} \cdot (\mathbf{a}_3^{(i)} - \mathbf{a}_3)\, \mathrm{d}S \right| \right) \\ &\leqslant \frac{C}{\sqrt{|\mathscr{E}|}} (\|\boldsymbol{\psi}_{\text{int}} \cdot \mathbf{a}_3\|_{0,\mathscr{E}} + h_{\mathscr{E}} \|\boldsymbol{\psi}_{\text{int}}\|_{0,\mathscr{E}}) \end{aligned} \tag{A.67}$$

since

$$\|\mathbf{a}_3^{(i)} - \mathbf{a}_3\|_{L^\infty(\mathscr{E})} \leqslant Ch_{\mathscr{E}} \tag{A.68}$$

Therefore, combining Equations (A.65)–(A.67), we get

$$\sup_i \|\boldsymbol{\psi}_{\text{int}}^{(i)} - \boldsymbol{\psi}_{\text{m}}^{(i)}\| \leqslant C(h_{\mathscr{E}}^{-1}\|\boldsymbol{\psi}_{\text{int}} \cdot \mathbf{a}_3\|_{0,\mathscr{E}} + \|\boldsymbol{\psi}_{\text{int}}\|_{1,\mathscr{E}}) \tag{A.69}$$

We now use Equation (A.64) twice consecutively to obtain first (A.57), then (A.56). We directly bound the right-hand side of Equation (A.64) by using (A.68) and (A.69). We first get

$$\begin{aligned}\|(\boldsymbol{\psi}_{\text{int}} - \mathscr{I}(\boldsymbol{\psi}_{\text{m}})) \cdot \mathbf{a}_3\|_{0,\mathscr{E}} &\leqslant C\sqrt{|\mathscr{E}|}\sup_i(\|\lambda_i\|_{L^\infty(\mathscr{E})}\|\boldsymbol{\psi}_{\text{int}}^{(i)} - \boldsymbol{\psi}_{\text{m}}^{(i)}\|\,\|\mathbf{a}_3^{(i)} - \mathbf{a}_3\|_{L^\infty(\mathscr{E})}) \\ &\leqslant C(h_{\mathscr{E}}\|\boldsymbol{\psi}_{\text{int}} \cdot \mathbf{a}_3\|_{0,\mathscr{E}} + h_{\mathscr{E}}^2\|\boldsymbol{\psi}_{\text{int}}\|_{1,\mathscr{E}})\end{aligned} \tag{A.70}$$

Combining this bound with Equations (A.58) and (A.63), we have

$$\|\boldsymbol{\psi}_{\text{int}} \cdot \mathbf{a}_3\|_{0,\mathscr{E}} \leqslant C(h_{\mathscr{E}}\|\boldsymbol{\psi}_{\text{int}} \cdot \mathbf{a}_3\|_{0,\mathscr{E}} + h_{\mathscr{E}}^2\|\boldsymbol{\psi}_{\text{int}}\|_{1,\mathscr{E}}) \tag{A.71}$$

Hence, for h small enough,

$$\|\boldsymbol{\psi}_{\text{int}} \cdot \mathbf{a}_3\|_{0,\mathscr{E}} \leqslant Ch_{\mathscr{E}}^2\|\boldsymbol{\psi}_{\text{int}}\|_{1,\mathscr{E}} \tag{A.72}$$

and, squaring this inequality and summing over all elements, we get (A.57).

We then use (A.64) again to bound the H^1 semi-norm.

$$\begin{aligned}&|\boldsymbol{\psi}_{\text{int}} - \mathscr{I}(\boldsymbol{\psi}_{\text{m}})) \cdot \mathbf{a}_3|_{1,\mathscr{E}} \\ &\quad\leqslant C\sqrt{|\mathscr{E}|}\sup_i \|\boldsymbol{\psi}_{\text{int}}^{(i)} - \boldsymbol{\psi}_{\text{m}}^{(i)}\|(\|\lambda_i\|_{W^{1,\infty}(\mathscr{E})}\|\mathbf{a}_3^{(i)} - \mathbf{a}_3\|_{L^\infty(\mathscr{E})} + \|\lambda_i\|_{L^\infty(\mathscr{E})}\|\mathbf{a}_3\|_{W^{1,\infty}(\mathscr{E})}) \\ &\quad\leqslant Ch_{\mathscr{E}}(h_{\mathscr{E}}^{-1}\|\boldsymbol{\psi}_{\text{int}} \cdot \mathbf{a}_3\|_{0,\mathscr{E}} + \|\boldsymbol{\psi}_{\text{int}}\|_{1,\mathscr{E}})(h_{\mathscr{E}}^{-1} \times h_{\mathscr{E}} + 1 \times 1) \\ &\quad\leqslant C(\|\boldsymbol{\psi}_{\text{int}} \cdot \mathbf{a}_3\|_{0,\mathscr{E}} + h_{\mathscr{E}}\|\boldsymbol{\psi}_{\text{int}}\|_{1,\mathscr{E}}) \\ &\quad\leqslant Ch_{\mathscr{E}}\|\boldsymbol{\psi}_{\text{int}}\|_{1,\mathscr{E}}\end{aligned} \tag{A.73}$$

using Equation (A.72). Finally, combining (A.73) with (A.58) and (A.63) we obtain

$$|\boldsymbol{\psi}_{\text{int}} \cdot \mathbf{a}_3|_{1,\mathscr{E}} \leqslant Ch_{\mathscr{E}}\|\boldsymbol{\psi}_{\text{int}}\|_{1,\mathscr{E}} \tag{A.74}$$

and Equation (A.56) immediately follows. □

Remark. It is easy to convince oneself, by considering specific examples where $\boldsymbol{\psi}_{\text{int}}$ is a nodal shape function on a curved surface, that the estimates in Equations (A.66) and (A.67) are optimal.

Lemma A.6 (*Consistency error*). *For any* $((\mathbf{v}, \boldsymbol{\psi}), (\mathbf{w}, \boldsymbol{\delta})) \in (\hat{\mathscr{U}}_h)^2$,

$$|\hat{A}(\mathbf{v}, \boldsymbol{\psi};\, \mathbf{w}, \boldsymbol{\delta}) - \hat{A}_h(\mathbf{v}, \boldsymbol{\psi};\, \mathbf{w}, \boldsymbol{\delta})| \leqslant Ch\|\mathbf{v}, \boldsymbol{\psi}\|_1\|\mathbf{w}, \boldsymbol{\delta}\|_1 \tag{A.75}$$

$$|\hat{F}(\mathbf{v}, \boldsymbol{\psi}) - \hat{F}_h(\mathbf{v}, \boldsymbol{\psi})| \leqslant Ch^2\|\mathbf{v}, \boldsymbol{\psi}\|_1 \tag{A.76}$$

Proof. From the definitions of $\hat{A}$ and $\hat{A}_h$ we have

$$\begin{aligned}
&|\hat{A}(\mathbf{v},\boldsymbol{\psi};\,\mathbf{w},\boldsymbol{\delta}) - \hat{A}_h(\mathbf{v},\boldsymbol{\psi};\,\mathbf{w},\boldsymbol{\delta})| \\
&\quad = |A^{(3D)}(\mathbf{v}+\xi_3\boldsymbol{\psi},\mathbf{w}+\xi_3\boldsymbol{\delta}) - \tilde{A}^{(3D)}(\mathbf{v}+\xi_3\mathscr{I}(\boldsymbol{\psi}),\mathbf{w}+\xi_3\mathscr{I}(\boldsymbol{\delta}))| \\
&\quad \leqslant |A^{(3D)}(\mathbf{v}+\xi_3\boldsymbol{\psi},\mathbf{w}+\xi_3\boldsymbol{\delta}) - A^{(3D)}(\mathbf{v}+\xi_3\mathscr{I}(\boldsymbol{\psi}),\mathbf{w}+\xi_3\mathscr{I}(\boldsymbol{\delta}))| \\
&\qquad + |A^{(3D)}(\mathbf{v}+\xi_3\mathscr{I}(\boldsymbol{\psi}),\mathbf{w}+\xi_3\mathscr{I}(\boldsymbol{\delta})) - \tilde{A}^{(3D)}(\mathbf{v}+\xi_3\mathscr{I}(\boldsymbol{\psi}),\mathbf{w}+\xi_3\mathscr{I}(\boldsymbol{\delta}))|
\end{aligned} \tag{A.77}$$

We now proceed to bound the two terms of the right-hand side separately,

$$\begin{aligned}
&|A^{(3D)}(\mathbf{v}+\xi_3\boldsymbol{\psi},\mathbf{w}+\xi_3\boldsymbol{\delta}) - A^{(3D)}(\mathbf{v}+\xi_3\mathscr{I}(\boldsymbol{\psi}),\mathbf{w}+\xi_3\mathscr{I}(\boldsymbol{\delta}))| \\
&\quad = |A^{(3D)}(\mathbf{v}+\xi_3\boldsymbol{\psi},\xi_3(\boldsymbol{\delta}-\mathscr{I}(\boldsymbol{\delta}))) + A^{(3D)}(\xi_3(\boldsymbol{\psi}-\mathscr{I}(\boldsymbol{\psi})),\mathbf{w}+\xi_3\mathscr{I}(\boldsymbol{\delta}))| \\
&\quad \leqslant C(\|\mathbf{v},\boldsymbol{\psi}\|_1\|\boldsymbol{\delta}-\mathscr{I}(\boldsymbol{\delta})\|_1 + \|\boldsymbol{\psi}-\mathscr{I}(\boldsymbol{\psi})\|_1\|\mathbf{w},\mathscr{I}(\boldsymbol{\delta})\|_1)
\end{aligned} \tag{A.78}$$

due to the boundedness of $A^{(3D)}$. Of course, the interpolation operator is continuous in $H^1(\Omega)$, so that

$$\|\mathscr{I}(\boldsymbol{\delta})\|_1 \leqslant C\|\boldsymbol{\delta}\|_1 \tag{A.79}$$

Furthermore, recalling (27), we have

$$\|\boldsymbol{\delta}-\mathscr{I}(\boldsymbol{\delta})\|_1 = \|\Pi\circ\mathscr{I}(\boldsymbol{\delta})-\mathscr{I}(\boldsymbol{\delta})\|_1 = \|\mathscr{I}(\boldsymbol{\delta})\cdot\mathbf{a}_3\|_1 \leqslant Ch\|\boldsymbol{\delta}\|_1 \tag{A.80}$$

from Lemma A.5, and the same holds for $\boldsymbol{\psi}$. Combining (A.78)–(A.80) we thus get

$$|A^{(3D)}(\mathbf{v}+\xi_3\boldsymbol{\psi},\mathbf{w}+\xi_3\boldsymbol{\delta}) - A^{(3D)}(\mathbf{v}+\xi_3\mathscr{I}(\boldsymbol{\psi}),\mathbf{w}+\xi_3\mathscr{I}(\boldsymbol{\delta}))| \leqslant Ch\|\mathbf{v},\boldsymbol{\psi}\|_1\|\mathbf{w},\boldsymbol{\delta}\|_1 \tag{A.81}$$

The second term on the right-hand side of Equation (A.77) represents the error due to the interpolation of the geometry. Note that the integrals involved in $A^{(3D)}$ and $\tilde{A}^{(3D)}$ are taken over the same domains, so that the only difference between the two expressions consists in using $\tilde{g}^{\alpha\beta}$ and $\tilde{g}$ in $\tilde{A}^{(3D)}$, instead of $g^{\alpha\beta}$ and g in $A^{(3D)}$, where the quantities with tilde signs are computed using the interpolated geometry given in Equation (23). Assuming sufficient regularity of the chart we have

$$\|\boldsymbol{\phi}-\mathscr{I}(\boldsymbol{\phi})\|_{W^{1,\infty}(\Omega)} \leqslant Ch^k \tag{A.82}$$

$$\|\mathbf{a}_3-\mathscr{I}(\mathbf{a}_3)\|_{W^{1,\infty}(\Omega)} \leqslant Ch^k \tag{A.83}$$

Hence

$$\tilde{g}^{\alpha\beta} = g^{\alpha\beta}(1+O(h^k)) \tag{A.84}$$

$$\sqrt{\tilde{g}} = \sqrt{g} + O(h^k) \tag{A.85}$$

Therefore

$$
\begin{aligned}
&|A^{(3D)}(\mathbf{v}+\xi_3\mathscr{I}(\boldsymbol{\psi}),\mathbf{w}+\xi_3\mathscr{I}(\boldsymbol{\delta}))-\tilde{A}^{(3D)}(\mathbf{v}+\xi_3\mathscr{I}(\boldsymbol{\psi}),\mathbf{w}+\xi_3\mathscr{I}(\boldsymbol{\delta}))|\\
&\quad\leqslant Ch^k\|\mathbf{v},\mathscr{I}(\boldsymbol{\psi})\|_1\|\mathbf{w},\mathscr{I}(\boldsymbol{\delta})\|_1\\
&\quad\leqslant Ch^k\|\mathbf{v},\boldsymbol{\psi}\|_1\|\mathbf{w},\boldsymbol{\delta}\|_1
\end{aligned}
\tag{A.86}
$$

Finally, combining (A.81) and (A.86), we get (A.75).

Similar arguments lead to Equation (A.76). The quadratic estimate is obtained from (A.57) since the expressions of $\hat{F}$ and $\hat{F}_h$ do not contain the derivatives of the displacements. □

Remark. The consistency error appears to be governed by the term in Equation (A.81), which is in $O(h)$ instead of the order of the finite element shape functions. To circumvent this difficulty, one can consider the shell finite element method obtained by dropping the interpolation operator in Equation (28). This amounts to using discrete displacements of the type

$$
\mathbf{U}_h=\sum_i\lambda_i(\xi_1,\xi_2)\mathbf{u}_h^{(i)}+\xi_3\Pi\left(\sum_i\lambda_i(\xi_1,\xi_2)\boldsymbol{\tau}_h^{(i)}\right) \tag{A.87}
$$

$$
\mathbf{V}=\sum_i\lambda_i(\xi_1,\xi_2)\mathbf{v}^{(i)}+\xi_3\Pi\left(\sum_i\lambda_i(\xi_1,\xi_2)\boldsymbol{\psi}^{(i)}\right) \tag{A.88}
$$

instead of those given in Equations (21) and (22). The consistency estimate for this modified procedure is then optimal.

Lemma A.7 (*Interpolation estimate*). *Assume* $(\mathbf{u},\boldsymbol{\tau})\in[H^{k+1}(\Omega)]^6$, *then*

$$
\|\mathbf{u}-\mathscr{I}(\mathbf{u}),\boldsymbol{\tau}-\Pi\circ\mathscr{I}(\boldsymbol{\tau})\|_1\leqslant Ch^k\|\mathbf{u},\boldsymbol{\tau}\|_{k+1} \tag{A.89}
$$

Proof. For $\mathbf{u}$, standard interpolation estimates directly give

$$
\|\mathbf{u}-\mathscr{I}(\mathbf{u})\|_1\leqslant Ch^k\|\mathbf{u}\|_{k+1} \tag{A.90}
$$

For $\boldsymbol{\tau}$ we have

$$
\|\boldsymbol{\tau}-\Pi\circ\mathscr{I}(\boldsymbol{\tau})\|_1=\|\Pi(\boldsymbol{\tau})-\Pi\circ\mathscr{I}(\boldsymbol{\tau})\|_1=\|\Pi(\boldsymbol{\tau}-\mathscr{I}(\boldsymbol{\tau}))\|_1\leqslant C\|\boldsymbol{\tau}-\mathscr{I}(\boldsymbol{\tau})\|_1\leqslant Ch^k\|\boldsymbol{\tau}\|_{k+1} \tag{A.91}
$$

□

We can now prove the final result of the paper.

Proof of Proposition 5.1 Note that $\hat{A}$ directly inherits the coercive and continuous character of A. Therefore, the consistency estimate (A.75) implies that $\hat{A}_h$ is continuous, and also coercive for h sufficiently small. Hence problem (28) is well-posed and has a unique solution.

Then, from the coercivity of $\hat{A}$, we have

$$\begin{aligned}
&\|\mathbf{u}_h - \mathscr{I}(\mathbf{u}), \boldsymbol{\tau}_h - \Pi \circ \mathscr{I}(\boldsymbol{\tau})\|_1^2 \\
&\quad \leqslant C\,\hat{A}(\mathbf{u}_h - \mathscr{I}(\mathbf{u}), \boldsymbol{\tau}_h - \Pi \circ \mathscr{I}(\boldsymbol{\tau}); \mathbf{u}_h - \mathscr{I}(\mathbf{u}), \boldsymbol{\tau}_h - \Pi \circ \mathscr{I}(\boldsymbol{\tau})) \\
&\quad = C[\,\hat{A}(\mathbf{u} - \mathscr{I}(\mathbf{u}), \boldsymbol{\tau} - \Pi \circ \mathscr{I}(\boldsymbol{\tau}); \mathbf{u}_h - \mathscr{I}(\mathbf{u}), \boldsymbol{\tau}_h - \Pi \circ \mathscr{I}(\boldsymbol{\tau})) \\
&\qquad + \hat{A}(\mathbf{u}_h, \boldsymbol{\tau}_h; \mathbf{u}_h - \mathscr{I}(\mathbf{u}), \boldsymbol{\tau}_h - \Pi \circ \mathscr{I}(\boldsymbol{\tau})) - \hat{A}(\mathbf{u}, \boldsymbol{\tau}; \mathbf{u}_h - \mathscr{I}(\mathbf{u}), \boldsymbol{\tau}_h - \Pi \circ \mathscr{I}(\boldsymbol{\tau}))] \\
&\quad = C[\,\hat{A}(\mathbf{u} - \mathscr{I}(\mathbf{u}), \boldsymbol{\tau} - \Pi \circ \mathscr{I}(\boldsymbol{\tau});\ \mathbf{u}_h - \mathscr{I}(\mathbf{u}), \boldsymbol{\tau}_h - \Pi \circ \mathscr{I}(\boldsymbol{\tau})) \\
&\qquad + \hat{A}(\mathbf{u}_h, \boldsymbol{\tau}_h;\ \mathbf{u}_h - \mathscr{I}(\mathbf{u}), \boldsymbol{\tau}_h - \Pi \circ \mathscr{I}(\boldsymbol{\tau})) - \hat{A}_h(\mathbf{u}_h, \boldsymbol{\tau}_h;\ \mathbf{u}_h - \mathscr{I}(\mathbf{u}), \boldsymbol{\tau}_h - \Pi \circ \mathscr{I}(\boldsymbol{\tau})) \\
&\qquad + \hat{F}_h(\mathbf{u}_h - \mathscr{I}(\mathbf{u}), \boldsymbol{\tau}_h - \Pi \circ \mathscr{I}(\boldsymbol{\tau})) - \hat{F}(\mathbf{u}_h - \mathscr{I}(\mathbf{u}), \boldsymbol{\tau}_h - \Pi \circ \mathscr{I}(\boldsymbol{\tau}))] \qquad \text{(A.92)}
\end{aligned}$$

using Equations (25) and (28) with $(\mathbf{v}, \boldsymbol{\psi}) = (\mathbf{u}_h - \mathscr{I}(\mathbf{u}), \boldsymbol{\tau}_h - \Pi \circ \mathscr{I}(\boldsymbol{\tau}))$. Hence, using the consistency estimates (A.75) and (A.76) together with the interpolation estimate (A.89) and the boundedness of $\hat{A}$, we get

$$\|\mathbf{u}_h - \mathscr{I}(\mathbf{u}), \boldsymbol{\tau}_h - \Pi \circ \mathscr{I}(\boldsymbol{\tau})\|_1^2 \leqslant C(h^k \|\mathbf{u}, \boldsymbol{\tau}\|_{k+1} + h\|\mathbf{u}_h, \boldsymbol{\tau}_h\|_1 + h^2)\|\mathbf{u}_h - \mathscr{I}(\mathbf{u}), \boldsymbol{\tau}_h - \Pi \circ \mathscr{I}(\boldsymbol{\tau})\|_1 \qquad \text{(A.93)}$$

The well-posedness of problem (28) implies that $\|\mathbf{u}_h, \boldsymbol{\tau}_h\|_1$ is uniformly bounded. Hence, simplifying (A.93) yields

$$\|\mathbf{u}_h - \mathscr{I}(\mathbf{u}), \boldsymbol{\tau}_h - \Pi \circ \mathscr{I}(\boldsymbol{\tau})\|_1 \leqslant Ch \qquad \text{(A.94)}$$

and a triangle inequality concludes the proof. □

REFERENCES

1. Bathe KJ. *Finite Element Procedures.* Prentice-Hall: Englewood Cliffs, NJ, 1996.
2. Bathe KJ, Chapelle D. *Finite Element Methods for Shells*, to appear.
3. Bernadou M. *Finite Element Methods for Thin Shell Problems*. Wiley: New York, 1996.
4. Zienkiewicz OC, Cheung YK. In *The Finite Element Method in Structural and Continuum Mechanics*. McGraw-Hill: New York, 1967; Zienkiewicz OC, Taylor RL. (4th edn.) vols. 1 and 2, 1989/1990.
5. Chapelle D, Bathe KJ. Fundamental considerations for the finite element analysis of shell problems. *Computers and Structures* 1998; **66**:19–36.
6. Bathe KJ, Iosilevich A, Chapelle D. An evaluation of the MITC shell elements. *Computers and Structures* 2000; **75**(1):1–30.
7. Bathe KJ, Iosilevich A, Chapelle D. An inf-sup test for shell finite elements. To appear in *Computers and Structures.*
8. Chapelle D, Bathe KJ. On general shell finite elements and mathematical shell models. In *Advances in Finite Element Procedures and Techniques*, Topping BHV (ed.). Civil-Comp Press: Edinburgh, Scotland, 1998.
9. Green AE, Zerna W. *Theoretical Elasticity* (2nd edn). Oxford University Press: Oxford, 1968.
10. Naghdi PM. Foundations of elastic shell theory. In *Progress in Solid Mechanics*, vol. 4. North-Holland: Amsterdam, 1963; 1–90.
11. Delfour M. Intrinsic differential geometric methods in the asymptotic analysis of linear thin shells. In *Boundaries, Interfaces and Transitions*, *CRM Proceedings and Lecture Notes*, vol. 13. American Mathematical Society: Providence, RI, 1998.
12. Ciarlet PG. *Introduction to Linear Shell Theory*, Series in Applied Mathematics. Gauthier-Villars: Paris; North-Holland: Amsterdam, 1998.
13. Chenais D, Paumier J.-C. On the locking phenomenon for a class of elliptic problems. *Numerische Mathematik* 1994; **67**:427–440.
14. Lions JL. *Perturbations Singulières dans les Problèmes aux Limites et en Contrôle Optimal.* Springer: Berlin, 1973.

